Computers and Mathematics with Applications 77 (2019) 2764–2785

Contents lists available at ScienceDirect

Computers and Mathematics with Applications

journal homepage: www.elsevier.com/locate/camwa

Divergence and flutter instabilities of nanobeams in moving state accounting for surface and shear effects

Keivan Kiani

Department of Civil Engineering, K.N. Toosi University of Technology, P.O. Box 15875-4416, Valiasr Ave., Tehran, Iran

ARTICLE INFO

Article history:
Received 23 July 2018
Received in revised form 19 December 2018
Accepted 10 January 2019
Available online 4 February 2019

Keywords:
Moving beam-like nanostructures
Transverse vibration
Surface effect
Shear deformable beam models
Dynamic instability
Galerkin approach

ABSTRACT

Transverse vibrations of elastically rested moving beam-like nanostructures accounting for surface effect are of high concern. The role of nonlocality on the free dynamic response of moving nanobeams has been revealed in recent years; nevertheless, the influence of the surface energy on the mechanical behavior of such elements has not been explained yet. In this paper, equations of motion of rested nanoscaled beams in the moving state are derived carefully via surface energetic-shear deformable beam models. Subsequently, the transverse vibrations of the nanostructure are evaluated using Galerkin-based assumed mode method. The explicit expressions of divergence velocities are obtained analytically, and these are successfully verified with the results of a numerical approach. The roles of crucial parameters on the first divergence velocity are addressed in some detail. Additionally, the stable and unstable regions are determined systematically and the influence of both surface energy and shear energy on the stability of moving nanostructure is discussed.

1. Introduction

To date, nano-scaled beam-like structures like nanowires have great potential applications in solar cells [1–3], lithium-ion batteries [4,5], nanoelectronic devices [6,7] including nanocircuits [8,9], and transistors [10,11]. For the case of using these nanodevices in high-speed carriers due to their high precision or when these tiny elements are subjected to movement due to externally applied forces, we should be aware of their vibrations and mechanical instabilities in the moving state. Given these potential applications and existing scientific gaps in the literature, herein, the author eagerly attempts to examine transverse vibrations and dynamic instabilities of moving nanoscaled-rested nanobeams using surface energetic beam models as a fundamental problem. Actually, this work could be considered as an essential step to encounter big challenges in the mechanical analysis of traveling double-nanobeam-systems or even ensembles of vertically aligned nanowires which are pivotal elements of the upcoming advanced technologies of the nano-electro-mechanical systems.

By decreasing the size of structures, the ratio of the surface area to the bulk volume increases, and thereby, the effect of surface energy on mechanical response becomes highlighted. One of the most popular elasticity-based theories in the modeling of the surface effect is that developed by Gurtin–Murdoch [12–14]. This theory explains that each solid continuum consists of two major parts: (i) surface layer with a negligible thickness, and (ii) its underlying bulk whose mechanical properties are different from those of the surface layer. The bulk is tightly bonded to the surface layer such that a perfect bond exists between them. It means that the displacement and stress fields of both surface layer and bulk are continuous at the interface. By assuming an isotropic surface layer, the strains within that are linked to the stresses via three surface constants, namely residual surface stress (τ_0) and two Lamé's parameters (λ_0 and μ_0). These factors are commonly determined by comparing the predicted results by the surface elasticity-based theory and those obtained from an appropriate atomic

E-mail address: k_kiani@kntu.ac.ir.

https://doi.org/10.1016/j.camwa.2019.01.008
0898-1221/

model [15,16]. In view of the above-mentioned continuities at the interface and by expressing the equations of motion for the surface layer and the bulk, these relations could be readily combined for rod-like, beam-like, and plate-like nanostructures. The main reason for this fact for the first ones is that the longitudinal strains in both surface layer and bulk are identical. Moreover, the reason for the latter two continuum-based nanostructures is that the transverse deflections do not vary across the thickness. As the beam-like nanostructure starts to move, not only the elastic strain energy of the surface layer, but also its kinetic energy contributes to the total potential energy of the moving nanostructure. The last contribution could play a critical role in dynamics and potential instability of the moving elastic nano-body which is attributed to the reduction of its lateral stiffness due to the centrifugal inertial effect. This matter has not been paid attention to by the scientific community until now. To bridge this gap, we employ Hamilton's principle by taking into account the potential energy of the surface layer accounting for both flexural and shear effects, and after that, the equations of motion of axially moving beam-like nanostructures are derived. The given studies and explorations in this article are associated with those that move along their major axis, however, this work could be generalized to the case of spatially moving nanostructures with three components of velocity.

At the atomic level, vibrations of each atom could influence the vibrations of its nearby atoms. Such a fact could not be tackled by the classical elasticity theory (CET) since it displays that the state of stress at each point only depends on the state of stress of that point. To overcome this shortcoming of the CET as well as considering nonlocality in field analysis at the nanoscale, nonlocal continuum theory was developed by Eringen [17,18]. Until now, a simple version of this theory (i.e., differential version) has been widely adopted by many researchers for vibrational scrutinies of nanobeams [19–21]. Further, an integral-based version (i.e., stress-driven formulation) has been of focus of attention for mechanical analysis of solids at small scales [22–27].

Up to now, the role of the surface energy on various aspects of mechanical behavior of nanoscaled beam-like structures has been investigated and displayed in the context of the surface elasticity theory (SET) of Gurtin–Murdoch [12–14]. For example, statics [28–31], linear vibrations [32–39], nonlinear vibrations [40–45], buckling [46–49], and postbuckling [50–52] of beam-like nanostructures accounting for the surface energy have been studied. A brief survey of the literature reveals that both linear and nonlinear transverse vibrations of moving macro-scaled beams have been examined [53–64]. Concerning the dynamic analysis of moving nanoscaled tubes and nanobeams, there exist several works on transverse vibrations [65–67] via nonlocal elasticity theory of Eringen. As it is seen, linear vibrations of elastic nanobeams with surface effect have not been explored yet. Further, the influence of the surface and shear deformation effects as well as their combinations on the mechanical response of moving nanostructures has not been displayed yet. In view of these scientific gaps and given the importance of the subject, the author has been encouraged to develop several inclusive models for axially moving beam-like-rested nanostructures accounting for both surface and shear effects.

Herein, free transverse vibrations of axially moving nanobeams are going to be studied in the context of the SET of Gurtin–Murdoch. By exploiting Rayleigh beam model (RBM), Timoshenko beam model (TBM), and higher-order beam model (HOBM), the equations of motion associated with the transverse vibration of the moving beam-like nanostructure are derived accounting for the surface energy by employing Hamilton's principle. By implementing the assumed mode method (AMM), the partial differential equations of motion of the suggested models are discretized in the spatial domain of the nanobeam. The resulted eigenvalue relations are solved for natural frequencies to determine the stable and unstable regions. The divergence and flutter instabilities are discussed and their corresponding velocities are evaluated both analytically and numerically. The influential factors on these crucial states are explained. Subsequently, the influence of surface and shear strain energies, nanobeam's length, and pretensioning force on the dominant flexural frequencies is explained for a wide range of the nanobeam's velocity.

2. Description of the nanomechanical problem

Consider an axially traveling beam-like nanostructure which is acted upon by a pretensioning force T_0 at its end, and rested on an elastic foundation (see Fig. 1). The nanobeam of concern is a uniformly circular solid structure of length l_b and its diameter is D_0. The elastically rested nanobeam is traveling with a constant velocity v_x. The interactions of the nanoscaled beam and the foundation have been modeled via continuous lateral and rotational springs of constants K_t and K_r, respectively. In the following, vibrations and dynamic instabilities of such a nanosystem, with emphasis on its transverse motion, are going to be examined using well-known surface energy-based beam theories.

3. Application of the surface energy-based RBM

3.1. Constitutive relations of the bulk and the surface layer

The RBM is mainly constructed based on this hypothesis that the perpendicular plane to the neutral axis remains plane after deformation. By excluding the longitudinal displacement of the neutral axis, the longitudinal and transverse displacement fields of the nanobeam could be expressed by: $u_x^R(x,y,z,t) = -z\frac{\partial w^R(x,t)}{\partial x}$, $u_z^R(x,y,z,t) = w^R(x,t)$, where z is the distance from the neutral axis, ∂ is the partial symbol, t is the time parameter, and $w^R = w^R(x,t)$ represents the deflection field of both bulk and surface layer. Throughout this article, the parameters with the superscripts R, T, and H in

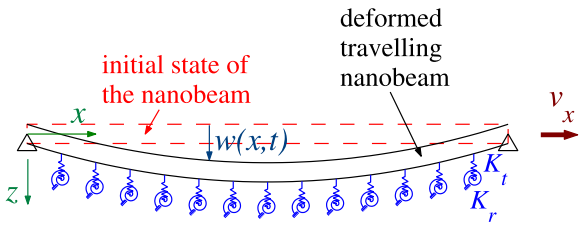

Fig. 1. A continuum-based representation of an axially moving nanoscaled beam rested on an elastic foundation.

order are associated with the RBM, TBM, and HOBM. In the framework of the small strains (i.e., $\epsilon_{ij}^R = \frac{1}{2}\left(\frac{\partial u_i^R}{\partial x_j} + \frac{\partial u_j^R}{\partial x_i}\right)$), the only non-vanishing strain of both bulk and surface layer is the longitudinal one which is stated by: $\epsilon_{xx}^R = -z\frac{\partial^2 w^R}{\partial x^2}$.

Using the surface elasticity theory of Gurtin–Murdoch [12–14], the only stresses within the surface layer are given by:

$$\tau_{xx}^R = \tau_0 + (\lambda_0 + 2\mu_0)\frac{\partial u_x^R}{\partial x} = \tau_0 - (\lambda_0 + 2\mu_0)\left(z\frac{\partial^2 w^R}{\partial x^2}\right), \quad \tau_{xz}^R = n_z\tau_0\frac{\partial w^R}{\partial x}, \tag{1}$$

where $\mathbf{n} = n_y\mathbf{e} + n_z\mathbf{e}_z$ is the unit normal vector to the surface layer, λ_0 and μ_0 are the Lamé's constants of the surface layer, and τ_0 is the residual stress within the surface layer under unrestrained conditions. The requirement of equilibrium of the surface layer at the farthest distance from the neutral axis reads [14,68]:

$$\begin{aligned} \tau_0\frac{\partial^2 u_z^{R,-}}{\partial x^2} + \sigma_{zz}^{R,-} &= \rho_0\frac{D^2 u_z^{R,-}}{Dt^2}, \quad z = -\frac{D_0}{2}, \\ \tau_0\frac{\partial^2 u_z^{R,+}}{\partial x^2} - \sigma_{zz}^{R,+} &= \rho_0\frac{D^2 u_z^{R,+}}{Dt^2}, \quad z = +\frac{D_0}{2}, \end{aligned} \tag{2}$$

where ρ_0 is the density of the surface layer, $\frac{D}{Dt}$ is the material derivative, $u_z^{R,-} = u_z^R(x, y, z = -\frac{D_0}{2}, t)$ and $u_z^{R,+} = u_z^R(x, y, z = \frac{D_0}{2}, t)$. By assuming this fact that the transverse normal stress of the bulk (σ_{zz}^R) would linearly vary between its corresponding surface values at the bottom and the top [69], namely $\sigma_{zz}^R = \left(\sigma_{zz}^{R,+} + \sigma_{zz}^{R,-}\right)/2 + z\left(\sigma_{zz}^{R,+} - \sigma_{zz}^{R,-}\right)/D_0$, and through using Eq. (2), it is obtainable:

$$\sigma_{zz}^R = \frac{2z}{D_0}\left[\tau_0\frac{\partial^2 w^R}{\partial x^2} - \rho_0\left(\frac{\partial^2 w^R}{\partial t^2} + 2v_x\frac{\partial^2 w^R}{\partial x\partial t} + v_x^2\frac{\partial^2 w^R}{\partial x^2}\right)\right]. \tag{3}$$

Additionally, the longitudinal normal stress within the bulk is stated by: $\sigma_{xx}^R = E_b\epsilon_{xx}^R + \nu_b\sigma_{zz}^R$. By substituting longitudinal strain–deflection relation and Eq. (3) to the recent relation, the longitudinal stress–deflection in moving surface energetic nanobeams takes the following form:

$$\sigma_{xx}^R = z\left[\left(\frac{2\nu_b\tau_0}{D_0} - E_b\right)\frac{\partial^2 w^R}{\partial x^2} - \frac{2\nu_b\rho_0}{D_0}\left(\frac{\partial^2 w^R}{\partial t^2} + 2v_x\frac{\partial^2 w^R}{\partial x\partial t} + v_x^2\frac{\partial^2 w^R}{\partial x^2}\right)\right]. \tag{4}$$

3.2. The governing equations using the surface energetic RBM

The kinetic energy (T^R) as well as the elastic strain energy of the rested-moving nanobeam (U^R) in which modeled based on the surface energy-based RBM are written as:

$$T^R(t) = \frac{1}{2}\int_\Omega\left[\rho_b\left(\left(\frac{Du_x^R}{Dt}\right)^2 + \left(\frac{Du_z^R}{Dt}\right)^2\right)\right]\mathrm{d}\Omega + \frac{1}{2}\int_{\mathcal{A}}\rho_0\left(\left(\frac{Du_x^R}{Dt}\right)^2 + \left(\frac{Du_z^R}{Dt}\right)^2\right)\mathrm{d}\mathcal{A}, \tag{5a}$$

$$\begin{aligned} U^R(t) = {} & \frac{1}{2}\int_\Omega\sigma_{xx}^R\epsilon_{xx}^R\,\mathrm{d}\Omega + \frac{1}{2}\int_{\mathcal{A}}\tau_{xx}^R\epsilon_{xx}^R\,\mathrm{d}\mathcal{A} + \frac{1}{2}\int_0^{l_b}(T_0 + \tau_0 S_0)\left(\frac{\partial w^R}{\partial x}\right)^2\mathrm{d}x \\ & + \frac{1}{2}\int_0^{l_b}\left(K_t\left(w^R\right)^2 + K_r\left(\frac{\partial w^R}{\partial x}\right)^2\right)\mathrm{d}x, \end{aligned} \tag{5b}$$

where $S_0 = \int_{\mathcal{S}} n_z^2\mathrm{d}\mathcal{S}$, Ω denotes the whole bulk domain of the moving nanobeam, $\mathcal{A}$ represents the surface layer domain, $\mathrm{d}\Omega$ and $\mathrm{d}\mathcal{A}$ are infinitesimal volume and area of the bulk and the surface layer, respectively, and for the problem at hand, the first material derivative is given by: $\frac{D[.]}{Dt} = \frac{\partial[.]}{\partial t} + v_x\frac{\partial[.]}{\partial x}$. By substituting Eqs. (1), (4), and the longitudinal strain expression

into Eqs. (5a) and (5b), the more detailed statements of kinetic and elastic strain energy of the moving nanostructure in terms of deformation fields are derived as:

$$T^R(t)=\int_0^{l_b}\left[(\rho_bA_b+\rho_0S_0)\left(\frac{\partial w^R}{\partial t}+v_x\frac{\partial w^R}{\partial x}\right)^2+(\rho_bI_b+\rho_0I_0)\left(\frac{\partial^3 w^R}{\partial x^2\partial t}+v_x\frac{\partial^3 w^R}{\partial x^3}\right)^2\right]\mathrm{d}x, \tag{6a}$$

$$U^R(t)=\frac{1}{2}\int_0^{l_b}\left\{\begin{array}{l} I_b\left[\left(\frac{2\nu_b\tau_0}{D_0}-E_b\right)\frac{\partial^2 w^R}{\partial x^2}-\frac{2\nu_b\rho_0}{D_0}\left(\frac{\partial^2 w^R}{\partial t^2}+2v_x\frac{\partial^2 w^R}{\partial x\partial t}+v_x^2\frac{\partial^2 w^R}{\partial x^2}\right)\right]\frac{\partial^2 w^R}{\partial x^2}+\\ I_0\left(\lambda_0+\mu_0\right)\left(\frac{\partial^2 w}{\partial x^2}\right)^2+K_t\left(w^R\right)^2+\left(K_r+\tau_0S_0+T_0\right)\left(\frac{\partial w^R}{\partial x}\right)^2 \end{array}\right\}\mathrm{d}x. \tag{6b}$$

Using Hamilton's principle and Eqs. (6a) and (6b), the equation of motion which describes transverse vibration of the axially moving nanobeam on the basis of the surface energetic RBM would take the following form:

$$\begin{aligned}&(\rho_bA_b+\rho_0S_0)\left(\frac{\partial^2 w^R}{\partial t^2}+2v_x\frac{\partial^2 w^R}{\partial x\partial t}+v_x^2\frac{\partial^2 w^R}{\partial x^2}\right)-\left(\rho_bI_b+\rho_0I_0-\frac{2\rho_0\nu_bI_b}{D_0}\right)\times\\&\left(\frac{\partial^4 w^R}{\partial t^2\partial x^2}+2v_x\frac{\partial^4 w^R}{\partial x^3\partial t}+v_x^2\frac{\partial^4 w^R}{\partial x^4}\right)+K_t\,w^R-(K_r+\tau_0S_0)\frac{\partial^2 w^R}{\partial x^2}\\&+\left(E_bI_b+(\lambda_0+2\mu_0)I_0-\frac{2\nu_b\tau_0I_b}{D_0}\right)\frac{\partial^4 w^R}{\partial x^4}=0.\end{aligned} \tag{7}$$

To facilitate studying the problem at hand, the following dimensionless parameters are considered:

$$\begin{aligned}&\overline{w}^R=\frac{w^R}{l_b},\ \xi=\frac{x}{l_b},\ \tau=\frac{t}{l_b^2}\sqrt{\frac{E_bI_b}{\rho_bA_b}},\ \lambda=\frac{l_b}{\sqrt{I_b/A_b}},\ \overline{T}_0^R=\frac{T_0l_b^2}{E_bI_b},\ \overline{K}_t^R=\frac{K_tl_b^4}{E_bI_b},\ \overline{K}_r^R=\frac{K_rl_b^2}{E_bI_b},\\&\chi_1^R=\frac{\rho_0S_0}{\rho_bA_b},\ \chi_2^R=\frac{\rho_0I_0}{\rho_bI_b}-\frac{2\nu_b\rho_0}{D_0\rho_b},\ \chi_3^R=\frac{(\lambda_0+2\mu_0)I_0}{E_bI_b}-\frac{2\nu_b\tau_0}{D_0E_b},\ \chi_4^R=\frac{\tau_0S_0l_b^2}{E_bI_b},\end{aligned} \tag{8}$$

hence, the dimensionless governing equation of an axially moving nanobeam based on the RBM is obtained as:

$$\begin{aligned}&\overline{\Upsilon}^R\left\{\left(1+\chi_1^R\right)\overline{w}^R-\lambda^{-2}\left(1+\chi_2^R\right)\frac{\partial^2\overline{w}^R}{\partial\xi^2}\right\}+\\&\left(1+\chi_3^R\right)\frac{\partial^4\overline{w}^R}{\partial\xi^4}-\left(\chi_4^R+\overline{K}_r^R+\overline{T}_0^R\right)\frac{\partial^2\overline{w}^R}{\partial\xi^2}+\overline{K}_t^R\overline{w}^R=0.\end{aligned} \tag{9}$$

where $\overline{\Upsilon}^R[.]=\frac{\partial^2[.]}{\partial\tau^2}+2\lambda\beta^R\frac{\partial^2[.]}{\partial\tau\partial\xi}+(\lambda\beta^R)^2\frac{\partial^2[.]}{\partial\xi^2}$ is a dimensionless operator.

It is very difficult, if impossible, to find an analytical solution to Eq. (9). To overcome this difficulty, a Galerkin-based AMM is suggested in the next part.

3.3. Spatial discretization using Galerkin-based AMM

Let,

$$\overline{w}^R(\xi,\tau)=\sum_{i=1}^{NM}\phi_i^w(\xi)\overline{w}_i^R(\tau), \tag{10}$$

where NM is the number of modes, $\phi_i^w(\xi)$ is the ith mode shape, and $\overline{w}_i^R(\tau)$ is the time-dependent parameter. Let us multiply both sides of Eq. (9) by $\delta\overline{w}^R$, δ is the variational symbol, taking the integral in the dimensionless spatial domain (i.e., [0,1]), and then, using the integration by parts technique, it is obtainable:

$$[\overline{\mathbf{M}}_b^R]^{ww}\frac{\mathrm{d}^2\overline{\mathbf{w}}^R}{\mathrm{d}\tau^2}+[\overline{\mathbf{C}}_b^R]^{ww}\frac{\mathrm{d}\overline{\mathbf{w}}^R}{\mathrm{d}\tau}+[\overline{\mathbf{K}}_b^R]^{ww}\,\overline{\mathbf{w}}^R=\mathbf{0}, \tag{11}$$

where

$$\left[\overline{\mathbf{M}}_b^R\right]_{ij}^{ww}=\int_0^1\left(\left(1+\chi_1^R\right)\phi_i^w\phi_j^w+\lambda^{-2}\left(1+\chi_2^R\right)\frac{\mathrm{d}\phi_i^w}{\mathrm{d}\xi}\frac{\mathrm{d}\phi_j^w}{\mathrm{d}\xi}\right)\mathrm{d}\xi, \tag{12a}$$

$$\left[\overline{\mathbf{C}}_b^R\right]_{ij}^{ww}=\int_0^1 2\lambda\beta^R\phi_i^w\left(\left(1+\chi_1^R\right)\frac{\mathrm{d}\phi_j^w}{\mathrm{d}\xi}-\lambda^{-2}\left(1+\chi_2^R\right)\frac{\mathrm{d}^3\phi_j^w}{\mathrm{d}\xi^3}\right)\mathrm{d}\xi, \tag{12b}$$

$$\left[\overline{\mathbf{K}}_b^R\right]_{ij}^{ww} = \int_0^1 \begin{pmatrix} \left(1+\chi_3^R\right)\dfrac{\mathrm{d}^2\phi_i^w}{\mathrm{d}\xi^2}\dfrac{\mathrm{d}^2\phi_j^w}{\mathrm{d}\xi^2} + \left(\chi_4^R+\overline{K}_r^R+\overline{T}_0^R\right)\dfrac{\mathrm{d}\phi_i^w}{\mathrm{d}\xi}\dfrac{\mathrm{d}\phi_j^w}{\mathrm{d}\xi} + \overline{K}_t^R\phi_i^w\phi_j^w \\ +\left(\lambda\beta^R\right)^2\phi_i^w\left(\left(1+\chi_1^R\right)\dfrac{\mathrm{d}^2\phi_j^w}{\mathrm{d}\xi^2} - \lambda^{-2}\left(1+\chi_2^R\right)\dfrac{\mathrm{d}^4\phi_j^w}{\mathrm{d}\xi^4}\right) \end{pmatrix} \mathrm{d}\xi, \tag{12c}$$

$$\overline{\mathbf{w}}^R(\tau) = \langle \overline{w}_1^R(\tau), \overline{w}_2^R(\tau), \ldots, \overline{w}_{NM}^R(\tau)\rangle^{\mathrm{T}}. \tag{12d}$$

4. Application of the surface energy-based TBM

4.1. Constitutive relations of the bulk and the surface layer

The chief privilege of the TBM over the RBM is in considering the shear effect. In the context of the TBM, the deflection and angle of rotation are essentially two distinct fields and such a consideration would let us incorporate the shear deformation effect into the formulations of the problem. Basically, Timoshenko [70] constructed his beam theory based on the following deformation fields: $u_x^T(x,y,z,t) = -z\theta^T(x,t)$ and $u_z^T(x,y,z,t) = w^T(x,t)$ in which θ^T denotes the angle of rotation about the y axis. By assuming small deflections, the non-vanishing components of the strains of both bulk and the surface layer would be:

$$\epsilon_{xx}^T = -z\frac{\partial\theta^T}{\partial x},\ \gamma_{xz}^T = \frac{\partial w^T}{\partial x} - \theta^T. \tag{13}$$

Using surface elasticity theory of Gurtin–Murdoch [12–14], the longitudinal normal stress and the shear stress of the surface layer are expressed by:

$$\tau_{xx}^T = \tau_0 + (\lambda_0+2\mu_0)\frac{\partial u_x^T}{\partial x} = \tau_0 - (\lambda_0+2\mu_0)\,z\frac{\partial\theta^T}{\partial x},\ \ \tau_{xz}^T = n_z\tau_0\frac{\partial w^T}{\partial x}. \tag{14}$$

On the other hand, the equations of motion of the bottom and the top surface layers in the transverse direction are provided by:

$$\begin{aligned} &\tau_0\frac{\partial^2 u_z^{T,-}}{\partial x^2} + \sigma_{zz}^{T,-} = \rho_0\frac{D^2u_z^{T,-}}{Dt^2},\ \ z = -\frac{D_0}{2},\\ &\tau_0\frac{\partial^2 u_z^{T,+}}{\partial x^2} - \sigma_{zz}^{T,+} = \rho_0\frac{D^2u_z^{T,+}}{Dt^2},\ \ z = +\frac{D_0}{2}, \end{aligned} \tag{15}$$

by assuming a linear variation of the normal stress along the z-direction within the bulk across the nanobeam's thickness, it is derived:

$$\sigma_{zz}^T = \frac{2z}{D_0}\left[\tau_0\frac{\partial^2 w^T}{\partial x^2} - \rho_0\left(\frac{\partial^2 w^T}{\partial t^2} + 2v_x\frac{\partial^2 w^T}{\partial x\partial t} + v_x^2\frac{\partial^2 w^T}{\partial x^2}\right)\right]. \tag{16}$$

Thereby, the longitudinal normal stress of the bulk (σ_{xx}^T) could be evaluated by:

$$\sigma_{xx}^T = E_b\epsilon_{xx}^T + \nu_b\sigma_{zz}^T = z\left\{-E_b\frac{\partial\theta^T}{\partial x} + \frac{2\nu_b}{D_0}\left[\tau_0\frac{\partial^2 w^T}{\partial x^2} - \rho_0\left(\frac{\partial^2 w^T}{\partial t^2} + 2v_x\frac{\partial^2 w^T}{\partial t\partial x} + v_x^2\frac{\partial^2 w^T}{\partial x^2}\right)\right]\right\}, \tag{17}$$

and the only shear stress within the bulk is given by:

$$\sigma_{xz}^T = k_s G_b\left(\frac{\partial w^T}{\partial x} - \theta^T\right), \tag{18}$$

where k_s is the shear correction factor.

4.2. The governing equations using the surface energetic TBM

The kinetic energy (T^T) and the elastic strain energy (U^T) of the elastically confined moving nanobeam accounting for the surface energy are stated by:

$$T^T(t) = \frac{1}{2}\int_\Omega\left[\rho_b\left(\left(\frac{Du_x^T}{Dt}\right)^2 + \left(\frac{Du_z^T}{Dt}\right)^2\right)\right]\mathrm{d}\Omega + \frac{1}{2}\int_{\mathcal{A}}\rho_0\left(\left(\frac{Du_x^T}{Dt}\right)^2 + \left(\frac{Du_z^T}{Dt}\right)^2\right)\mathrm{d}\mathcal{A}, \tag{19a}$$

$$\begin{aligned} U^T(t) = \ & \frac{1}{2}\int_\Omega\left(\sigma_{xx}^T\epsilon_{xx}^T + \sigma_{xz}^T\gamma_{xz}^T\right)\mathrm{d}\Omega + \frac{1}{2}\int_{\mathcal{A}}\left(\tau_{xx}^T\epsilon_{xx}^T + \tau_{xz}^T\gamma_{xz}^T\right)\mathrm{d}\mathcal{A} + \\ & \frac{1}{2}\int_0^{l_b}(T_0+\tau_0S_0)\left(\frac{\partial w^T}{\partial x}\right)^2\mathrm{d}x + \frac{1}{2}\int_0^{l_b}\left(K_t\left(w^T\right)^2 + K_r\left(\theta^T\right)^2\right)\mathrm{d}x, \end{aligned} \tag{19b}$$

by substituting Eqs. (13), (14), (17) and (18) into Eqs. (19a) and (19b), the kinetic and elastic strain energy of the axially moving nanobeam in terms of its deformation fields are stated by:

$$T^T(t)=\int_0^{l_b}\left[\begin{array}{l}(\rho_bA_b+\rho_0S_0)\left(\dfrac{\partial w^T}{\partial t}+v_x\dfrac{\partial w^T}{\partial x}\right)^2+\\ (\rho_bI_b+\rho_0I_0)\left(\dfrac{\partial \theta^T}{\partial t}+v_x\dfrac{\partial \theta^T}{\partial x}\right)^2\end{array}\right]\mathrm{d}x, \tag{20a}$$

$$U^T(t)=\frac{1}{2}\int_0^{l_b}\left\{\begin{array}{l}I_b\left(-E_b\dfrac{\partial \theta^T}{\partial x}+\dfrac{2\nu_b}{D_0}\left(\tau_0\dfrac{\partial^2 w^T}{\partial x^2}-\rho_0\left(\dfrac{\partial^2 w^T}{\partial t^2}+2v_x\dfrac{\partial^2 w^T}{\partial t\partial x}+v_x^2\dfrac{\partial^2 w^T}{\partial x^2}\right)\right)\right)\times\\ \dfrac{\partial \theta^T}{\partial x}+k_sG_bA_b\left(\dfrac{\partial w^T}{\partial x}-\theta^T\right)^2+I_0\left(\lambda_0+\mu_0\right)\left(\dfrac{\partial \theta^T}{\partial x}\right)^2+\\ (T_0+\tau_0S_0)\left(\dfrac{\partial w^T}{\partial x}\right)^2+K_t\left(w^T\right)^2+K_r\left(\theta^T\right)^2\end{array}\right\}\mathrm{d}x. \tag{20b}$$

By employing the Hamilton's principle, the surface energetic transverse equations of motion of the moving nanostructure on the basis of the TBM are obtained as:

$$\begin{array}{l}(\rho_bI_b+\rho_0I_0)\left(\dfrac{\partial^2\theta^T}{\partial t^2}+2v_x\dfrac{\partial^2\theta^T}{\partial t\partial x}+v_x^2\dfrac{\partial^2\theta^T}{\partial x^2}\right)-\dfrac{2\nu_bI_b\rho_0}{D_0}\left(\dfrac{\partial^3 w^T}{\partial t^2\partial x}+2v_x\dfrac{\partial^3 w^T}{\partial t\partial x^2}+v_x^2\dfrac{\partial^3 w^T}{\partial x^3}\right)\\ +\dfrac{2\nu_bI_b\tau_0}{D_0}\dfrac{\partial^3 w^T}{\partial x^3}-k_sG_bA_b\left(\dfrac{\partial w^T}{\partial x}-\theta^T\right)-\left(E_bI_b+\left(\lambda_0+2\mu_0\right)I_0\right)\dfrac{\partial^2\theta^T}{\partial x^2}+k_r\,\theta^T=0,\end{array} \tag{21a}$$

$$\begin{array}{l}(\rho_bA_b+\rho_0S_0)\left(\dfrac{\partial^2 w^T}{\partial t^2}+2v_x\dfrac{\partial^2 w^T}{\partial t\partial x}+v_x^2\dfrac{\partial^2 w^T}{\partial x^2}\right)\\ -k_sG_bA_b\left(\dfrac{\partial^2 w^T}{\partial x^2}-\dfrac{\partial\theta^T}{\partial x}\right)-(T_0+\tau_0S_0)\dfrac{\partial^2 w^T}{\partial x^2}+K_t\,w^T=0.\end{array} \tag{21b}$$

By considering the following dimensionless quantities,

$$\begin{array}{l}\overline{w}^T=\dfrac{w^T}{l_b},\ \overline{\theta}^T=\theta^T,\ \tau=\dfrac{t}{l_b}\sqrt{\dfrac{G_b}{\rho_b}},\ \eta=\dfrac{E_bI_b}{k_sG_bA_bl_b^2},\ \beta^T=\dfrac{v_x}{\sqrt{\frac{k_sG_b}{\rho_b}}},\\ \overline{K}_t^T=\dfrac{K_tl_b^2}{k_sG_bA_b},\ \overline{K}_r^T=\dfrac{K_r}{k_sG_bA_b},\ \overline{T}_0^T=\dfrac{T_0}{k_sG_bA_b},\ \chi_1^T=\dfrac{\rho_0S_0}{\rho_bA_b},\ \chi_2^T=\dfrac{\rho_0I_0}{\rho_bI_b},\\ \chi_3^T=\dfrac{2\nu_b\rho_0}{\rho_bD_0},\ \chi_4^T=\dfrac{2\nu_bI_b\tau_0}{k_sG_bA_bl_b^2D_0},\ \chi_5^T=\dfrac{(\lambda_0+2\mu_0)I}{k_sG_bAb_bl_b^2},\ \chi_6^T=\dfrac{\tau_0S_0}{k_sG_bA_b},\end{array} \tag{22}$$

one can arrive at the dimensionless equations of motion of the axially moving nanobeam with surface energy:

$$\begin{array}{l}\overline{\Upsilon}^T\left\{\lambda^{-2}\left(1+\chi_2^T\right)\overline{\theta}^T-\lambda^{-2}\chi_3^T\dfrac{\partial\overline{w}^T}{\partial\xi}\right\}+\chi_4^T\dfrac{\partial^3\overline{w}^T}{\partial\xi^3}-\\ \left(\eta+\chi_5^T\right)\dfrac{\partial^2\overline{\theta}^T}{\partial\xi^2}-\left(\dfrac{\partial\overline{w}^T}{\partial\xi}-\overline{\theta}^T\right)+\overline{K}_r^T\overline{\theta}^T=0,\end{array} \tag{23a}$$

$$\overline{\Upsilon}^T\left\{\left(1+\chi_1^T\right)\overline{w}^T\right\}-\left(\frac{\partial^2\overline{w}^T}{\partial\xi^2}-\frac{\partial\overline{\theta}^T}{\partial\xi}\right)-\left(\overline{T}_0^T+\chi_6^T\right)\frac{\partial^2\overline{w}^T}{\partial\xi^2}+\overline{K}_t^T\overline{w}^T=0, \tag{23b}$$

where the dimensionless operator in Eqs. (23a) and (23b) is defined by:

$$\overline{\Upsilon}^T[.]=\frac{\partial^2[.]}{\partial\tau^2}+2\beta^T\frac{\partial^2[.]}{\partial\tau\partial\xi}+\beta^2\frac{\partial^2[.]}{\partial\xi^2}. \tag{24}$$

4.3. Spatial discretization using Galerkin-based AMM

Let us consider:

$$\overline{w}^T(\xi,\tau)=\sum_{i=1}^{NM}\phi_i^w(\xi)\overline{w}_i^T(\tau),\ \ \overline{\theta}^T(\xi,\tau)=\sum_{i=1}^{NM}\phi_i^\theta(\xi)\overline{\theta}_i^T(\tau). \tag{25}$$

where ϕ_i^w and ϕ_i^θ are the mode shapes associated with the deflection and the angle of deflection, respectively, and $\overline{w}_i^T$ and $\overline{\theta}_i^T$ are their corresponding time-dependent factors. By premultiplying both sides of Eqs. (23a) and (23b) by $\delta\overline{\theta}^T$ and $\delta\overline{w}^T$, and then integrating over [0,1], through taking the necessary integration by parts, one can arrive at the following second-order ordinary differential equations:

$$\begin{bmatrix} [\overline{\mathbf{M}}_b^T]^{\theta\theta} & [\overline{\mathbf{M}}_b^T]^{\theta w} \\ [\overline{\mathbf{M}}_b^T]^{w\theta} & [\overline{\mathbf{M}}_b^T]^{ww} \end{bmatrix} \begin{Bmatrix} \dfrac{\mathrm{d}^2\overline{\boldsymbol{\Theta}}^T}{\mathrm{d}\tau^2} \\ \dfrac{\mathrm{d}^2\overline{\mathbf{w}}^T}{\mathrm{d}\tau^2} \end{Bmatrix} + \begin{bmatrix} [\overline{\mathbf{C}}_b^T]^{\theta\theta} & [\overline{\mathbf{C}}_b^T]^{\theta w} \\ [\overline{\mathbf{C}}_b^T]^{w\theta} & [\overline{\mathbf{C}}_b^T]^{ww} \end{bmatrix} \begin{Bmatrix} \dfrac{\mathrm{d}\overline{\boldsymbol{\Theta}}^T}{\mathrm{d}\tau} \\ \dfrac{\mathrm{d}\overline{\mathbf{w}}^T}{\mathrm{d}\tau} \end{Bmatrix}$$
$$\begin{bmatrix} [\overline{\mathbf{K}}_b^T]^{\theta\theta} & [\overline{\mathbf{K}}_b^T]^{\theta w} \\ [\overline{\mathbf{K}}_b^T]^{w\theta} & [\overline{\mathbf{K}}_b^T]^{ww} \end{bmatrix} \begin{Bmatrix} \overline{\boldsymbol{\Theta}}^T \\ \overline{\mathbf{w}}^T \end{Bmatrix} = \begin{Bmatrix} \mathbf{0} \\ \mathbf{0} \end{Bmatrix}, \tag{26}$$

where the non-vanishing submatrices are as:

$$\left[\overline{\mathbf{M}}_b^T\right]_{ij}^{\theta\theta} = \int_0^1 \lambda^{-2}\left(1+\chi_2^T\right)\phi_i^\theta\phi_j^\theta \mathrm{d}\xi, \tag{27a}$$

$$\left[\overline{\mathbf{M}}_b^T\right]_{ij}^{\theta w} = \int_0^1 \lambda^{-2}\chi_3^T\frac{\mathrm{d}\phi_i^\theta}{\mathrm{d}\xi}\phi_j^w \mathrm{d}\xi, \tag{27b}$$

$$\left[\overline{\mathbf{M}}_b^T\right]_{ij}^{ww} = \int_0^1 \left(1+\chi_1^T\right)\phi_i^w\phi_j^w \mathrm{d}\xi, \tag{27c}$$

$$\left[\overline{\mathbf{C}}_b^T\right]_{ij}^{\theta\theta} = \int_0^1 2\lambda^{-2}\beta^T\left(1+\chi_2^T\right)\phi_i^\theta\frac{\mathrm{d}\phi_j^\theta}{\mathrm{d}\xi}\,\mathrm{d}\xi, \tag{27d}$$

$$\left[\overline{\mathbf{C}}_b^T\right]_{ij}^{\theta w} = -\int_0^1 2\lambda^{-2}\beta^T\,\chi_3^T\phi_i^\theta\frac{\mathrm{d}^2\phi_j^w}{\mathrm{d}\xi}\mathrm{d}\xi, \tag{27e}$$

$$\left[\overline{\mathbf{C}}_b^T\right]_{ij}^{ww} = \int_0^1 2\beta^T\left(1+\chi_1^T\right)\phi_i^w\frac{\mathrm{d}\phi_j^w}{\mathrm{d}\xi}\mathrm{d}\xi, \tag{27f}$$

$$\left[\overline{\mathbf{K}}_b^T\right]_{ij}^{\theta\theta} = \int_0^1 \left(\left(1+\overline{K}_r^T\right)\phi_i^\theta\phi_j^\theta + \left(\eta+\chi_5^T\right)\frac{\mathrm{d}\phi_i^\theta}{\mathrm{d}\xi}\frac{\mathrm{d}\phi_j^\theta}{\mathrm{d}\xi} + \left(1+\chi_2^T\right)\left(\frac{\beta^T}{\lambda}\right)^2\phi_i^\theta\frac{\mathrm{d}^2\phi_j^\theta}{\mathrm{d}\xi^2}\right)\mathrm{d}\xi, \tag{27g}$$

$$\left[\overline{\mathbf{K}}_b^T\right]_{ij}^{\theta w} = \int_0^1 \left(-\left(\phi_i^\theta\frac{\mathrm{d}\phi_j^w}{\mathrm{d}\xi} + \chi_4^T\frac{\mathrm{d}\phi_i^\theta}{\mathrm{d}\xi}\frac{\mathrm{d}^2\phi_j^w}{\mathrm{d}\xi^2}\right) + \chi_3^T\left(\frac{\beta^T}{\lambda}\right)^2\frac{\mathrm{d}^3\phi_i^\theta}{\mathrm{d}\xi^3}\phi_j^w\right)\mathrm{d}\xi, \tag{27h}$$

$$\left[\overline{\mathbf{K}}_b^T\right]_{ij}^{w\theta} = -\int_0^1 \frac{\mathrm{d}\phi_i^w}{\mathrm{d}\xi}\phi_j^\theta\,\mathrm{d}\xi, \tag{27i}$$

$$\left[\overline{\mathbf{K}}_b^T\right]_{ij}^{ww} = \int_0^1 \left(\left(1+\chi_6^T+\overline{T}_0^T\right)\frac{\mathrm{d}\phi_i^w}{\mathrm{d}\xi}\frac{\mathrm{d}\phi_j^w}{\mathrm{d}\xi} + \left(1+\chi_1^T\right)\left(\beta^T\right)^2\phi_i^w\frac{\mathrm{d}^2\phi_j^w}{\mathrm{d}\xi^2} + \overline{K}_t^T\phi_i^w\phi_j^w\right)\mathrm{d}\xi, \tag{27j}$$

$$\overline{\boldsymbol{\Theta}}^T(\tau) = \langle\overline{\theta}_1^T(\tau), \overline{\theta}_2^T(\tau), \ldots, \overline{\theta}_{NM}^T(\tau)\rangle^{\mathrm{T}}, \tag{27k}$$

$$\overline{\mathbf{w}}^T(\tau) = \langle\overline{w}_1^T(\tau), \overline{w}_2^T(\tau), \ldots, \overline{w}_{NM}^T(\tau)\rangle^{\mathrm{T}}. \tag{27l}$$

5. Application of the surface energy-based HOBM

5.1. Constitutive relations of the bulk and the surface layer

As it is seen, the TBM provides a more rational model with respect to the RBM to include shear deformation in the formulations. However, the TBM would not guarantee zero shear stress at the bottom and top surfaces of the nanobeam.

For more accurate estimation of shear effect, Bickford [71] and Reddy [72,73] proposed a HOBM to conquer this drawback of the TBM. In the context of this HOBM, the displacement fields of both bulk and surface layer are expressed by:

$$u_x^H(x,y,z,t) = -\left[\left(z-\alpha z^3\right)\psi^H(x,t) + \alpha z^3 \frac{\partial w^H}{\partial x}(x,t)\right],\quad u_z^H(x,y,z,t) = w^H(x,t), \tag{28}$$

where $\alpha = 4/(3D_0^2)$, $\psi^H = \psi^H(x,t)$ is the angle of rotation field about the y axis, and $w^H = w^H(x,t)$ is the transverse displacement along the z axis. Thereby, the non-vanishing shear strains are as:

$$\epsilon_{xx}^H = -\left[\left(z-\alpha z^3\right)\frac{\partial \psi^H}{\partial x} + \alpha z^3 \frac{\partial^2 w^H}{\partial x^2}\right],\quad \gamma_{xz}^H = \left(1-3\alpha z^2\right)\left(\frac{\partial w^H}{\partial x} - \psi^H\right). \tag{29}$$

The only surface stresses on the basis of the surface elasticity theory of the Gurtin–Murdoch [12–14] are given as follows:

$$\tau_{xx}^H = \tau_0 - (\lambda_0 + 2\mu_0)\left[\left(z-\alpha z^3\right)\frac{\partial \psi^H}{\partial x} + \alpha z^3 \frac{\partial^2 w^H}{\partial x^2}\right],\quad \tau_{xz}^H = n_z \tau_0 \frac{\partial w^H}{\partial x}. \tag{30}$$

The requirement of equilibrium of the bottom and the top surface layer in the transverse direction yields:

$$\begin{aligned} &\tau_0 \frac{\partial^2 u_z^{H,-}}{\partial x^2} + \sigma_{zz}^{H,-} = \rho_0 \frac{D^2 u_z^{H,-}}{Dt^2},\quad z = -\frac{D_0}{2},\\ &\tau_0 \frac{\partial^2 u_z^{H,+}}{\partial x^2} - \sigma_{zz}^{H,+} = \rho_0 \frac{D^2 u_z^{H,+}}{Dt^2},\quad z = +\frac{D_0}{2}, \end{aligned} \tag{31}$$

where $u_z^{H,-} = u_z^H(x,y,z=-\frac{D_0}{2},t)$, $u_z^{H,+} = u_z^H(x,y,z=\frac{D_0}{2},t)$, $\sigma_{zz}^{H,-} = \sigma_{zz}^H(x,y,z=-\frac{D_0}{2},t)$, and $\sigma_{zz}^{H,+} = \sigma_{zz}^H(x,y,z=\frac{D_0}{2},t)$. If σ_{zz}^H within the bulk varies linearly between those corresponding values at the bottom and top, in view of Eqs. (31)(a) and (31)(b), it is readily obtainable:

$$\sigma_{zz}^H = \frac{2z}{D_0}\left(\tau_0 \frac{\partial^2 w^H}{\partial x^2} - \rho_0\left(\frac{\partial^2 w^H}{\partial t^2} + 2v_x \frac{\partial^2 w^H}{\partial t \partial x} + v_x^2 \frac{\partial^2 w^H}{\partial x^2}\right)\right). \tag{32}$$

By virtue of $\sigma_{xx}^H = E_b \epsilon_{xx}^H + \nu_b \sigma_{zz}^H$ through exploiting Eqs. (29) and (32), the longitudinal stress within the bulk of the axially moving nanobeam is stated by:

$$\begin{aligned} \sigma_{xx}^H = \; & -E_b\left[\left(z-\alpha z^3\right)\frac{\partial \psi^H}{\partial x} + \alpha z^3 \frac{\partial^2 w^H}{\partial x^2}\right] + \\ & \frac{2\nu_b}{D_0}\left[z\left(\tau_0 \frac{\partial^2 w^H}{\partial x^2} - \rho_0\left(\frac{\partial^2 w^H}{\partial t^2} + 2v_x \frac{\partial^2 w^H}{\partial t \partial x} + v_x^2 \frac{\partial^2 w^H}{\partial x^2}\right)\right)\right], \end{aligned} \tag{33}$$

and in view of the given shear strains in Eq. (29), the only shear stress of the bulk is evaluated as follows:

$$\sigma_{xz}^H = \left(1-3\alpha z^2\right) G_b \left(\frac{\partial w^H}{\partial x} - \psi^H\right). \tag{34}$$

5.2. The governing equations using the surface energetic HOBM

The kinetic energy (T^H) and the elastic strain energy of the axially moving nanobeam (U^H) modeled according to the HOBM are evaluated as:

$$T^H(t) = \frac{1}{2}\int_\Omega \rho_b \left(\left(\frac{Du_x^H}{Dt}\right)^2 + \left(\frac{Du_z^H}{Dt}\right)^2\right) \mathrm{d}\Omega + \frac{1}{2}\int_{\mathcal{A}} \rho_0 \left(\left(\frac{Du_x^H}{Dt}\right)^2 + \left(\frac{Du_z^H}{Dt}\right)^2\right) \mathrm{d}\mathcal{A}, \tag{35a}$$

$$\begin{aligned} U^H(t) = \; & \frac{1}{2}\int_\Omega \left(\sigma_{xx}^H \epsilon_{xx}^H + \sigma_{xz}^H \gamma_{xz}^H\right) \mathrm{d}\Omega + \frac{1}{2}\int_{\mathcal{A}} \left(\tau_{xx}^H \epsilon_{xx}^H + \tau_{xz}^H \gamma_{xz}^H\right) \mathrm{d}\mathcal{A} + \\ & \frac{1}{2}\int_0^{l_b} (T_0 + \tau_0 S_0)\left(\frac{\partial w^H}{\partial x}\right)^2 \mathrm{d}x + \frac{1}{2}\int_0^{l_b} \left(K_t \left(w^H\right)^2 + K_r \left(\psi^H\right)^2\right) \mathrm{d}x, \end{aligned} \tag{35b}$$

by introducing Eqs. (30), (33), and (34) to Eqs. (35a) and (35b),

$$T^H = \frac{1}{2}\int_0^{l_b} \left(\begin{array}{l} \left(I_0 + I_0^*\right)\left(\frac{\partial^2 w^H}{\partial t \partial x} + v_x \frac{\partial^2 w^H}{\partial x^2}\right)^2 + \left(I_2 + I_2^*\right)\left(\frac{\partial \psi^H}{\partial t} + v_x \frac{\partial \psi^H}{\partial x}\right)^2 + \\ \alpha^2\left(I_6 + I_6^*\right)\left(\frac{\partial \psi^H}{\partial t} + \frac{\partial^2 w^H}{\partial t \partial x} + v_x\left(\frac{\partial \psi^H}{\partial x} + \frac{\partial^2 w^H}{\partial x^2}\right)\right)^2 \\ -2\alpha\left(I_4 + I_4^*\right)\left(\frac{\partial \psi^H}{\partial t} + v_x \frac{\partial \psi^H}{\partial x}\right)\left(\frac{\partial \psi^H}{\partial t} + \frac{\partial^2 w^H}{\partial t \partial x} + v_x\left(\frac{\partial \psi^H}{\partial x} + \frac{\partial^2 w^H}{\partial x^2}\right)\right) \end{array}\right) \mathrm{d}x, \tag{36a}$$

$$U^H = \frac{1}{2}\int_0^{l_b}\begin{pmatrix}\dfrac{\partial\psi^H}{\partial x}M_b^H + \left(\psi^H + \dfrac{\partial w^H}{\partial x}\right)\left(\alpha\,\dfrac{\partial P_b^H}{\partial x} + Q_b^H\right)\\ K_t\left(w^H\right)^2 + K_r\left(\psi^H\right)^2 + (T_0+\tau_0 S_0)\left(\dfrac{\partial w^H}{\partial x}\right)^2\end{pmatrix}\mathrm{d}x + \frac{1}{2}\int_0^{l_b}\int_{\mathcal{S}}\begin{pmatrix}\tau_{xx}^H\epsilon_{xx}^H +\\ \tau_{xz}^H\gamma_{xz}^H\end{pmatrix}\mathrm{d}\mathcal{S}\mathrm{d}x, \tag{36b}$$

where

$$M_b^H = -\left[(J_2-\alpha J_4)\,\frac{\partial\psi^H}{\partial x} + \alpha J_4\frac{\partial^2 w^H}{\partial x^2}\right] + \frac{2\nu_b I_2'}{D_0}\left(\tau_0\frac{\partial^2 w^H}{\partial x^2} - \rho_0\left(\frac{\partial^2 w^H}{\partial t^2} + 2v_x\frac{\partial^2 w^H}{\partial t\partial x} + v_x^2\frac{\partial^2 w^H}{\partial x^2}\right)\right), \tag{37a}$$

$$P_b^H = -\left[(J_4-\alpha J_6)\,\frac{\partial\psi^H}{\partial x} + \alpha J_6\frac{\partial^2 w^H}{\partial x^2}\right] + \frac{2\nu_b I_4'}{D_0}\left(\tau_0\frac{\partial^2 w^H}{\partial x^2} - \rho_0\left(\frac{\partial^2 w^H}{\partial t^2} + 2v_x\frac{\partial^2 w^H}{\partial t\partial x} + v_x^2\frac{\partial^2 w^H}{\partial x^2}\right)\right), \tag{37b}$$

$$Q_b^H = \kappa\left(\frac{\partial w^H}{\partial x} - \psi^H\right), \tag{37c}$$

and

$$\begin{aligned}&\kappa = \int_{A_b} G_b\left(1-3\alpha z^2\right)\mathrm{d}A,\ I_m' = \int_{A_b} z^m\,\mathrm{d}A,\ I_m'^* = \int_{\mathcal{S}} z^m\,\mathrm{d}\mathcal{S};\ m=2,4,\\ &J_n = \int_{A_b} E_b z^n\,\mathrm{d}A,\ I_n = \int_{A_b}\rho_b z^n\,\mathrm{d}A,\ I_n^* = \int_{\mathcal{S}}\rho_0 z^n\,\mathrm{d}\mathcal{S};\ n=0,2,4,6.\end{aligned} \tag{38}$$

By exploiting Hamilton's principle, the transverse equations of motion of the moving nanostructure modeled by the higher-order beam are derived as:

$$\begin{aligned}&\left(\left(I_2+I_2^*\right)-2\alpha\left(I_4+I_4^*\right)+\alpha^2\left(I_6+I_6^*\right)\right)\left(\frac{\partial^2\psi^H}{\partial t^2}+2v_x\frac{\partial^2\psi^H}{\partial t\partial x}+v_x^2\frac{\partial^2\psi^H}{\partial x^2}\right)+\\ &\left(\alpha^2\left(I_6+I_6^*\right)-\alpha\left(I_4+I_4^*\right)\right)\left(\frac{\partial^3 w^H}{\partial t^2\partial x}+2v_x\frac{\partial^3 w^H}{\partial t\partial x^2}+v_x^2\frac{\partial^3 w^H}{\partial x^3}\right)+\\ &-\frac{\partial M_b^H}{\partial x}+\alpha\frac{\partial P_b^H}{\partial x}+Q_b^H-\int_{\mathcal{S}} z\,\frac{\partial\tau_{xx}^H}{\partial x}\,\mathrm{d}\mathcal{S}-K_r\psi^H=0,\end{aligned} \tag{39a}$$

$$\begin{aligned}&\left(I_0+I_0^*\right)\left(\frac{\partial^2 w^H}{\partial t^2}+2v_x\frac{\partial^2 w^H}{\partial t\partial x}+v_x^2\frac{\partial^2 w^H}{\partial x^2}\right)+\\ &\left(\alpha I_4-\alpha^2 I_6\right)\left(\frac{\partial^3\psi^H}{\partial t^2\partial x}+2v_x\frac{\partial^3\psi^H}{\partial t\partial x^2}+v_x^2\frac{\partial^3\psi^H}{\partial x^3}\right)\\ &-\frac{\partial Q_{b_z}^H}{\partial x}-\alpha\frac{\partial^2 P_{b_z}^H}{\partial x^2}-\int_{\mathcal{S}}\frac{\partial\tau_{xz}^H}{\partial x}n_z\,\mathrm{d}\mathcal{S}+(T_0+\tau_0 S_0)\,\frac{\partial^2 w^H}{\partial x^2}+K_t w^H=0.\end{aligned} \tag{39b}$$

To study vibrations of moving nanobeams in a more general framework via HOBM, we consider the following dimensionless quantities:

$$\begin{aligned}&\overline{v}^H=\frac{v^H}{l_b},\ \overline{w}^H=\frac{w^H}{l_b},\ \overline{\psi}_y^H=\psi^H,\ \overline{\psi}_z^H=\psi_z^H,\ \tau=\frac{\alpha t}{l_b^2}\sqrt{\frac{J_6}{I_0}},\ \gamma_1^2=\frac{\alpha I_4-\alpha^2 I_6}{I_0 l_b^2},\\ &\gamma_2^2=\frac{\alpha^2 I_6}{I_0 l_b^2},\ \gamma_3^2=\frac{\kappa l_b^2}{\alpha^2 J_6},\ \gamma_4^2=\frac{\alpha J_4-\alpha^2 J_6}{\alpha^2 J_6},\ \gamma_6^2=\frac{\alpha I_4-\alpha^2 I_6}{I_2-2\alpha I_4+\alpha^2 I_6},\end{aligned}$$

$$
\begin{aligned}
&\gamma_7^2 = \frac{\kappa I_0 I_b^4}{(I_2 - 2\alpha I_4 + \alpha^2 I_6)\alpha^2 J_6},\ \gamma_8^2 = \frac{(J_2 - 2\alpha J_4 + \alpha^2 J_6) I_0 I_b^2}{(I_2 - 2\alpha I_4 + \alpha^2 I_6)\alpha^2 J_6},\ \gamma_9^2 = \frac{(\alpha J_4 - \alpha^2 J_6) I_0 I_b^2}{(I_2 - 2\alpha I_4 + \alpha^2 I_6)\alpha^2 J_6},\\
&\overline{K}_t^H = \frac{K_t I_b^4}{\alpha^2 J_6},\ \overline{K}_r^H = \frac{K_r I_0 I_b^4}{(I_2 - 2\alpha I_4 + \alpha^2 I_6)\alpha^2 J_6},\ \overline{T}_0^H = \frac{T_0 I_b^3}{\alpha^2 J_6},\\
&\chi_1^H = \frac{I_2^* - 2\alpha I_4^* + \alpha^2 I_6^*}{I_2 - 2\alpha I_4 + \alpha^2 I_6},\ \chi_2^H = \frac{\alpha I_4^* - \alpha^2 I_6^* - \frac{2\nu_b \rho_0}{D_0}\left(I_2' - \alpha I_4'\right)}{\alpha I_4 - \alpha^2 I_6},\\
&\chi_3^H = \frac{(\lambda_0 + 2\mu_0) - \frac{2\nu_b \tau_0}{D_0}\left(I_2' - \alpha I_4'\right)}{\alpha J_4 - \alpha^2 J_6},\ \chi_4^H = \frac{(\lambda_0 + 2\mu_0)\left(I_2^* - \alpha I_4^*\right)}{J_2 - 2\alpha J_4 + \alpha^2 J_6},\\
&\chi_5^H = \frac{\rho_0 S_0 + \frac{2\alpha \nu_b I_4' \rho_0}{D_0}}{I_0},\ \chi_6^H = \frac{\tau_0 S_0 I_b^3}{\alpha^2 J_6},\ \chi_7^H = \frac{2\nu_b I_4' \tau_0 I_b^3}{\alpha J_6 D_0}.
\end{aligned}
\tag{40}
$$

By introducing Eqs. (30), (37a)–(37c) to Eqs. (39a) and (39b), in view of Eq. (40), the dimensionless equations of motion that display transverse vibrations of surface energetic moving nanobeams on the basis of the HOBM are obtained as follows:

$$
\begin{aligned}
&\overline{\Upsilon}^H \left\{ \left(1 + \chi_1^H\right) \partial^2 \overline{\psi}^H + \gamma_6^2 \left(1 + \chi_2^H\right) \frac{\partial \overline{w}^H}{\partial \xi} \right\} - \gamma_9^2 \left(1 + \chi_3^H\right) \frac{\partial^3 \overline{w}^H}{\partial \xi^3}\\
&-\gamma_8^2 \left(1 + \chi_4^H\right) \frac{\partial^2 \overline{\psi}^H}{\partial \xi^2} - \gamma_7^2 \left(\frac{\partial \overline{w}^H}{\partial \xi} - \overline{\psi}^H \right) + \overline{K}_r^H \overline{\psi}^H = 0,
\end{aligned}
\tag{41a}
$$

$$
\begin{aligned}
&\overline{\Upsilon}^H \left\{ \left(1 + \chi_5^H\right) \partial^2 \overline{w}^H - \gamma_2^2 \frac{\partial^2 \overline{w}^H}{\partial \xi^2} + \gamma_1^2 \frac{\partial \overline{\psi}^H}{\partial \xi} \right\} - \gamma_3^2 \left(\frac{\partial^2 \overline{w}^H}{\partial \xi^2} - \frac{\partial \overline{\psi}^H}{\partial \xi} \right)\\
&- \left(\overline{T}_0^H + \chi_6^H \right) \frac{\partial^2 \overline{w}^H}{\partial \xi^2} + \gamma_4^2 \frac{\partial^3 \overline{\psi}^H}{\partial \xi^3} + \left(1 - \chi_7^H\right) \frac{\partial^4 \overline{w}^H}{\partial \xi^4} + \overline{K}_t^H \overline{w}^H = 0,
\end{aligned}
\tag{41b}
$$

where

$$
\overline{\Upsilon}^H [.] = \frac{\partial^2 [.]}{\partial \tau^2} + 2\beta^H \frac{\partial^2 [.]}{\partial \tau \partial \xi} + \left(\beta^H\right)^2 \frac{\partial^2 [.]}{\partial \xi^2}. \tag{42}
$$

5.3. Spatial discretization using Galerkin-based AMM

Let

$$
\overline{w}^H(\xi, \tau) = \sum_{i=1}^{NM} \phi_i^w(\xi) \overline{w}_i^H(\tau),\ \ \overline{\psi}^H(\xi, \tau) = \sum_{i=1}^{NM} \phi_i^\psi(\xi) \overline{\psi}_i^H(\tau), \tag{43}
$$

by premultiplying both sides of Eqs. (41a) and (41b) by $\delta\overline{\psi}^H$ and $\delta\overline{w}^H$, respectively, and integrating over $[0, 1]$ through taking the required integration by parts, it is derived:

$$
\begin{aligned}
&\begin{bmatrix} [\overline{\mathbf{M}}_b^H]^{\psi\psi} & [\overline{\mathbf{M}}_b^H]^{\psi w} \\ [\overline{\mathbf{M}}_b^H]^{w\psi} & [\overline{\mathbf{M}}_b^H]^{ww} \end{bmatrix} \begin{Bmatrix} \frac{\mathrm{d}^2 \overline{\mathbf{\Psi}}^H}{\mathrm{d}\tau^2} \\ \frac{\mathrm{d}^2 \overline{\mathbf{w}}^H}{\mathrm{d}\tau^2} \end{Bmatrix} + \begin{bmatrix} [\overline{\mathbf{C}}_b^H]^{\psi\psi} & [\overline{\mathbf{C}}_b^H]^{\psi w} \\ [\overline{\mathbf{C}}_b^H]^{w\psi} & [\overline{\mathbf{C}}_b^H]^{ww} \end{bmatrix} \begin{Bmatrix} \frac{\mathrm{d}\overline{\mathbf{\Psi}}^H}{\mathrm{d}\tau} \\ \frac{\mathrm{d}\overline{\mathbf{w}}^H}{\mathrm{d}\tau} \end{Bmatrix}\\
&\begin{bmatrix} [\overline{\mathbf{K}}_b^H]^{\psi\psi} & [\overline{\mathbf{K}}_b^H]^{\psi w} \\ [\overline{\mathbf{K}}_b^H]^{w\psi} & [\overline{\mathbf{K}}_b^H]^{ww} \end{bmatrix} \begin{Bmatrix} \overline{\mathbf{\Psi}}^H \\ \overline{\mathbf{w}}^H \end{Bmatrix} = \begin{Bmatrix} \mathbf{0} \\ \mathbf{0} \end{Bmatrix},
\end{aligned}
\tag{44}
$$

where,

$$
\left[\overline{\mathbf{M}}_b^H\right]_{ij}^{\psi\psi} = \int_0^1 \left(1 + \chi_1^H\right) \phi_i^\psi \phi_j^\psi \mathrm{d}\xi, \tag{45a}
$$

$$
\left[\overline{\mathbf{M}}_b^H\right]_{ij}^{\psi w} = \int_0^1 \gamma_6^2 \left(1 + \chi_2^H\right) \phi_i^\psi \frac{\mathrm{d}\phi_j^w}{\mathrm{d}\xi} \mathrm{d}\xi, \tag{45b}
$$

$$
\left[\overline{\mathbf{M}}_b^H\right]_{ij}^{w\psi} = -\int_0^1 \gamma_1^2 \frac{\mathrm{d}\phi_i^w}{\mathrm{d}\xi} \phi_j^\psi \mathrm{d}\xi, \tag{45c}
$$

$$\left[\overline{\mathbf{M}}_b^H\right]_{ij}^{ww} = \int_0^1 \left(\left(1+\chi_5^H\right)\phi_i^w\phi_j^w + \gamma_2^2 \frac{\mathrm{d}\phi_i^w}{\mathrm{d}\xi}\frac{\mathrm{d}\phi_j^w}{\mathrm{d}\xi} \right) \mathrm{d}\xi, \tag{45d}$$

$$\left[\overline{\mathbf{C}}_b^H\right]_{ij}^{\psi\psi} = \int_0^1 2\beta^H \left(1+\chi_1^H\right)\phi_i^\psi \frac{\mathrm{d}\phi_j^\psi}{\mathrm{d}\xi}\mathrm{d}\xi, \tag{45e}$$

$$\left[\overline{\mathbf{C}}_b^H\right]_{ij}^{\psi w} = \int_0^1 2\beta^H\gamma_6^2 \left(1+\chi_2^H\right)\phi_i^\psi \frac{\mathrm{d}^2\phi_j^w}{\mathrm{d}\xi^2}\mathrm{d}\xi, \tag{45f}$$

$$\left[\overline{\mathbf{C}}_b^H\right]_{ij}^{w\psi} = -\int_0^1 2\beta^H\gamma_1^2 \frac{\mathrm{d}\phi_i^w}{\mathrm{d}\xi}\frac{\mathrm{d}\phi_j^w}{\mathrm{d}\xi}\mathrm{d}\xi, \tag{45g}$$

$$\left[\overline{\mathbf{C}}_b^H\right]_{ij}^{ww} = \int_0^1 2\beta^H \left(\left(1+\chi_5^H\right)\phi_i^w \frac{\mathrm{d}\phi_j^w}{\mathrm{d}\xi} + \gamma_2^2 \frac{\mathrm{d}\phi_i^w}{\mathrm{d}\xi}\frac{\mathrm{d}^2\phi_j^w}{\mathrm{d}\xi^2} \right) \mathrm{d}\xi, \tag{45h}$$

$$\left[\overline{\mathbf{K}}_b^H\right]_{ij}^{\psi\psi} = \int_0^1 \left(\begin{array}{l} \left(\overline{K}_r^H + \gamma_7^2\right)\phi_i^\psi\phi_j^\psi + \gamma_8^2\left(1+\chi_4^H\right)\dfrac{\mathrm{d}\phi_i^\psi}{\mathrm{d}\xi}\dfrac{\mathrm{d}\phi_j^\psi}{\mathrm{d}\xi} + \\ \left(\beta^H\right)^2\left(1+\chi_1^H\right)\phi_i^\psi\dfrac{\mathrm{d}^2\phi_j^\psi}{\mathrm{d}\xi^2} \end{array} \right) \mathrm{d}\xi, \tag{45i}$$

$$\left[\overline{\mathbf{K}}_b^H\right]_{ij}^{\psi w} = -\int_0^1 \left(\begin{array}{l} \gamma_7^2\phi_i^\psi\dfrac{\mathrm{d}\phi_j^w}{\mathrm{d}\xi} - \gamma_9^2\left(1+\chi_3^H\right)\dfrac{\mathrm{d}\phi_i^\psi}{\mathrm{d}\xi}\dfrac{\mathrm{d}^2\phi_j^w}{\mathrm{d}\xi^2} + \\ \left(\beta^H\right)^2\gamma_6^2\left(1+\chi_2^H\right)\phi_i^\psi\dfrac{\mathrm{d}^3\phi_j^w}{\mathrm{d}\xi^3} \end{array} \right) \mathrm{d}\xi, \tag{45j}$$

$$\left[\overline{\mathbf{K}}_b^H\right]_{ij}^{w\psi} = -\int_0^1 \left(\gamma_3^2\frac{\mathrm{d}\phi_i^w}{\mathrm{d}\xi}\phi_j^\psi - \gamma_4^2\frac{\mathrm{d}^2\phi_i^w}{\mathrm{d}\xi^2}\frac{\mathrm{d}\phi_j^\psi}{\mathrm{d}\xi} - \left(\beta^H\right)^2\gamma_1^2\frac{\mathrm{d}\phi_i^w}{\mathrm{d}\xi}\frac{\mathrm{d}^2\phi_j^\psi}{\mathrm{d}\xi^2} \right) \mathrm{d}\xi, \tag{45k}$$

$$\left[\overline{\mathbf{K}}_b^H\right]_{ij}^{ww} = \int_0^1 \left(\begin{array}{l} \left(\gamma_3^2 + \chi_6^H + \overline{T}_0^H\right)\dfrac{\mathrm{d}\phi_i^w}{\mathrm{d}\xi}\dfrac{\mathrm{d}\phi_j^w}{\mathrm{d}\xi} + \left(1-\chi_7^H\right)\dfrac{\mathrm{d}^2\phi_i^w}{\mathrm{d}\xi^2}\dfrac{\mathrm{d}^2\phi_j^w}{\mathrm{d}\xi^2} + \\ \overline{K}_t^H\phi_i^w\phi_j^w + \left(\beta^H\right)^2\left(\left(1+\chi_5^H\right)\phi_i^w\dfrac{\mathrm{d}^2\phi_j^w}{\mathrm{d}\xi^2} + \gamma_2^2\dfrac{\mathrm{d}\phi_i^w}{\mathrm{d}\xi}\dfrac{\mathrm{d}^3\phi_j^w}{\mathrm{d}\xi^3} \right) \end{array} \right) \mathrm{d}\xi, \tag{45l}$$

$$\overline{\mathbf{\Psi}}^H(\tau) = \langle \overline{\psi}_1^H(\tau), \overline{\psi}_2^H(\tau), \ldots, \overline{\psi}_{NM}^H(\tau)\rangle^{\mathrm{T}}, \tag{45m}$$

$$\overline{\mathbf{w}}^H(\tau) = \langle \overline{w}_1^H(\tau), \overline{w}_2^H(\tau), \ldots, \overline{w}_{NM}^H(\tau)\rangle^{\mathrm{T}}. \tag{45n}$$

6. Results and discussion

Consider a moving silver [001] nanobeam with the following properties [32,74]: $E_b = 76$ GPa, $\nu_b = 0.26$, $\rho_b = 10\,500$ kg/m^3, $\rho_0 = 10^{-7}$ kg/m^2, $\lambda_0 + 2\mu_0 = 1.22$ N/m, and $\tau_0 = 0.89$ N/m. We are interested in examining free vibration of such a nanostructure in moving state as well as explaining the interactional role of the velocity and the surface energy on its natural frequencies and stability.

In the following parts, a detailed scrutiny is provided to discuss on the roles of influential factors on the dynamic instability of the nanostructure and the divergence velocity. Via two methods, the divergence velocity of the nanostructure is evaluated and the capabilities of the suggested approaches are explained. Subsequently, the stable and unstable zones based on the proposed surface-energy-based models are revealed. More specifically, the effects of the velocity, length, and surface energy on the free dynamic response of the moving nanobeam are discussed. Further, the crucial roles of shear strain energy and surface effect on the obtained results are displayed in some detail.

6.1. Initiation of divergence instability

By increasing the axial velocity of the moving nanobeam, the natural frequencies of the nanostructure would generally lessen. At certain levels of velocities, which are called divergence ones, the frequencies would vanish, and instability would be generated within the moving nanobeam. By passing the velocity at the divergence level, the imaginary part of the frequency becomes negative and any cause of lateral displacement will cause divergence instability at which the amplitude of transverse displacement would magnify exponentially with time until resulting in structural failure. Therefore, a more accurate prediction of divergence velocities of various modes would be of great importance. In the following part, two methods are displayed to calculate such crucial parameters.

6.1.1. Analytical solution (AS)

Let us assume a harmonic form for time-dependent vectors of vibration modes of the suggested surface energetic models as in the following form:

$$\overline{\mathbf{w}}^{[.]}(\tau) = \overline{\mathbf{w}}_0^{[.]}\, e^{\mathrm{i}\varpi\tau},\quad \overline{\mathbf{\Theta}}^{T}(\tau) = \overline{\mathbf{\Theta}}_0^{T}\, e^{\mathrm{i}\varpi\tau},\quad \overline{\mathbf{\Psi}}^{H}(\tau) = \overline{\mathbf{\Psi}}_0^{H}\, e^{\mathrm{i}\varpi\tau};\ [.] = R, T, H, \tag{46}$$

where ϖ is the dimensionless frequency, $\overline{\mathbf{w}}_0^{[.]}$, $\overline{\mathbf{\Theta}}_0^{T}$, and $\overline{\mathbf{\Psi}}_0^{H}$ are the dimensionless amplitude vectors, and $\mathrm{i} = \sqrt{-1}$. By introducing Eq. (46) to Eqs. (11), (26), and (44), considering $\varpi = 0$ as the onset of the divergence instability, and neglecting the stiffness interactions of each pair of modes, it is obtainable:

$$[\overline{\mathbf{K}}_b^{R}]_{ii}^{ww}\, \overline{\mathbf{w}}_{0i}^{R} = \mathbf{0}, \tag{47a}$$

$$\begin{bmatrix} [\overline{\mathbf{K}}_b^{T}]_{ii}^{\theta\theta} & [\overline{\mathbf{K}}_b^{T}]_{ii}^{\theta w} \\ [\overline{\mathbf{K}}_b^{T}]_{ii}^{w\theta} & [\overline{\mathbf{K}}_b^{T}]_{ii}^{ww} \end{bmatrix} \begin{Bmatrix} \overline{\mathbf{\Theta}}_{0i}^{T} \\ \overline{\mathbf{w}}_{0i}^{T} \end{Bmatrix} = \begin{Bmatrix} 0 \\ 0 \end{Bmatrix}, \tag{47b}$$

$$\begin{bmatrix} [\overline{\mathbf{K}}_b^{H}]_{ii}^{\psi\psi} & [\overline{\mathbf{K}}_b^{H}]_{ii}^{\psi w} \\ [\overline{\mathbf{K}}_b^{H}]_{ii}^{w\psi} & [\overline{\mathbf{K}}_b^{H}]_{ii}^{ww} \end{bmatrix} \begin{Bmatrix} \overline{\mathbf{\Psi}}_{0i}^{H} \\ \overline{\mathbf{w}}_{0i}^{H} \end{Bmatrix} = \begin{Bmatrix} 0 \\ 0 \end{Bmatrix}. \tag{47c}$$

The requirement of the existence of a nontrivial solution to Eqs. (47a)–(47c) is that the determinant of the coefficient matrices associated with the amplitude vectors should be zero. Hence, by solving the following eigenvalue relations for β, the explicit expressions of dimensionless divergence velocities of the moving nanobeam based on the surface energetic models could be readily evaluated. Without loss of generality, we restrict our attention to the simply supported case. For this purpose, the following admissible mode shapes could be considered for all suggested models in this work:

$$\phi_i^{w} = \sin(i\pi\xi),\ \phi_i^{\theta} = \cos(i\pi\xi),\ \phi_i^{\psi} = \cos(i\pi\xi). \tag{48}$$

Therefore, the dimensionless divergence velocities of the mth flexural mode of the moving nanostructure based on the RBM, TBM, and HOBM are easily calculated as follows:

$$\left(\beta_m^{d}\right)^{R} = \sqrt{\frac{(m\pi)^4\left(1+\chi_3^{R}\right) + (m\pi)^2\left(\chi_4^{R} + \overline{T}_0^{R} + \overline{K}_r^{R}\right) + \overline{K}_t^{R}}{\lambda^2\,(m\pi)^2\left(1+\chi_1^{R}\right) + (m\pi)^4\left(1+\chi_2^{H}\right)}}, \tag{49a}$$

$$\left(\beta_m^{d}\right)^{T} = \sqrt{\frac{b_m^{T} - \sqrt{\left(b_m^{T}\right)^2 - 4a_m^{T}c_m^{T}}}{2a_m^{T}}}, \tag{49b}$$

$$\left(\beta_m^{d}\right)^{H} = \sqrt{\frac{b_m^{H} - \sqrt{\left(b_m^{H}\right)^2 - 4a_m^{H}c_m^{H}}}{2a_m^{H}}}, \tag{49c}$$

where $a_m^{[.]}$, $b_m^{[.]}$, and $c_m^{[.]}$ are given in Appendix A, and the dimensionless divergence velocities by the surface-energetic TBM and HOBM are stated in terms of dimensionless divergence velocity of the RBM (i.e., $\left(\beta_m^{*d}\right)^{R}$) as:

$$\left(\beta_m^{*d}\right)^{T} = \sqrt{\frac{E_b}{k_s G_b}}\,\left(\beta_m^{*d}\right)^{R},\quad \left(\beta_m^{*d}\right)^{H} = \frac{l_b}{\alpha}\sqrt{\frac{I_0 E_b}{\rho_b J_6}}\,\left(\beta_m^{*d}\right)^{R}. \tag{50}$$

It is worth mentioning that for very slender moving nanobeams, the rotary inertia effect could be safely ignored. In such a case, Eq. (49a) would be reduced to that predicted by the surface-energetic Euler–Bernoulli beam theory, namely:

$$\left(\beta_m^d\right)^E = \sqrt{\frac{(m\pi)^4\left(1+\chi_3^R\right)+(m\pi)^2\left(\chi_4^R+\overline{T}_0^R+\overline{K}_r^R\right)+\overline{K}_t^R}{\lambda^2(m\pi)^2\left(1+\chi_1^R\right)}}. \tag{51}$$

Both Euler–Bernoulli and Rayleigh beam models could not capture the shear divergence velocities due to their drawbacks in considering the shear strain energy. Nevertheless, the dimensionless divergence velocities of the mth mode of shear using the TBM and HOBM are calculated as:

$$\left(\beta_m^d\right)_{sh}^T = \sqrt{\frac{b_m^T+\sqrt{\left(b_m^T\right)^2-4a_m^Tc_m^T}}{2a_m^T}}, \tag{52a}$$

$$\left(\beta_m^d\right)_{sh}^H = \sqrt{\frac{b_m^H+\sqrt{\left(b_m^H\right)^2-4a_m^Hc_m^H}}{2a_m^H}}. \tag{52b}$$

6.1.2. Numerical solution (NS)

The main assumption in calculating the analytical divergence velocities of the previous part was to provoke the modes' interactions. To obtain more reasonable results as well as to check the accuracy of the analytical's results, a simple approach is developed. Actually, we are interested in establishing the eigenvalue relations using the Galerkin-based mass, damping, and stiffness matrices for the proposed models. Given Eqs. (11), (26), and (44), the onset of divergence instability is specified by $\varpi = 0$. Therefore, the following static eigenvalue relations are obtained for the suggested models:

$$[\overline{\mathbf{K}}_b^R]^{ww}\,\overline{\mathbf{w}}_0^R = \mathbf{0}, \tag{53a}$$

$$\begin{bmatrix}[\overline{\mathbf{K}}_b^T]^{\theta\theta} & [\overline{\mathbf{K}}_b^T]^{\theta w}\\ [\overline{\mathbf{K}}_b^T]^{w\theta} & [\overline{\mathbf{K}}_b^T]^{ww}\end{bmatrix}\begin{Bmatrix}\overline{\Theta}_0^T\\ \overline{\mathbf{w}}_0^T\end{Bmatrix} = \begin{Bmatrix}\mathbf{0}\\ \mathbf{0}\end{Bmatrix}, \tag{53b}$$

$$\begin{bmatrix}[\overline{\mathbf{K}}_b^H]^{\psi\psi} & [\overline{\mathbf{K}}_b^H]^{\psi w}\\ [\overline{\mathbf{K}}_b^H]^{w\psi} & [\overline{\mathbf{K}}_b^H]^{ww}\end{bmatrix}\begin{Bmatrix}\overline{\Psi}_0^H\\ \overline{\mathbf{w}}_0^H\end{Bmatrix} = \begin{Bmatrix}\mathbf{0}\\ \mathbf{0}\end{Bmatrix}. \tag{53c}$$

The non-trivial solutions would exist to Eq. (53) if and only if the determinant of the coefficients matrices associated with the constant vectors would be zero. Hence,

$$\det\left([\overline{\mathbf{K}}_{bs}^R]^{ww}-\left(\left(\beta^d\right)^R\right)^2[\overline{\mathbf{K}}_{bm}^R]^{ww}\right)=0, \tag{54a}$$

$$\det\left(\begin{bmatrix}[\overline{\mathbf{K}}_{bs}^T]^{\theta\theta} & [\overline{\mathbf{K}}_{bs}^T]^{\theta w}\\ [\overline{\mathbf{K}}_{bs}^T]^{w\theta} & [\overline{\mathbf{K}}_{bs}^T]^{ww}\end{bmatrix}-\left(\left(\beta^d\right)^T\right)^2\begin{bmatrix}[\overline{\mathbf{K}}_{bm}^T]^{\theta\theta} & [\overline{\mathbf{K}}_{bm}^T]^{\theta w}\\ [\overline{\mathbf{K}}_{bm}^T]^{w\theta} & [\overline{\mathbf{K}}_{bm}^T]^{ww}\end{bmatrix}\right)=0, \tag{54b}$$

$$\det\left(\begin{bmatrix}[\overline{\mathbf{K}}_{bs}^H]^{\psi\psi} & [\overline{\mathbf{K}}_{bs}^H]^{\psi w}\\ [\overline{\mathbf{K}}_{bs}^H]^{w\psi} & [\overline{\mathbf{K}}_{bs}^H]^{ww}\end{bmatrix}-\left(\left(\beta^d\right)^H\right)^2\begin{bmatrix}[\overline{\mathbf{K}}_{bm}^H]^{\psi\psi} & [\overline{\mathbf{K}}_{bm}^H]^{\psi w}\\ [\overline{\mathbf{K}}_{bm}^H]^{w\psi} & [\overline{\mathbf{K}}_{bm}^H]^{ww}\end{bmatrix}\right)=0, \tag{54c}$$

where $\left(\beta^d\right)^T = \sqrt{\frac{E_b}{k_sG_b}}\left(\beta^d\right)^R$ and $\left(\beta^d\right)^H = \frac{l_b}{\alpha}\sqrt{\frac{l_0E_b}{\rho_bJ_6}}\left(\beta^d\right)^R$, and the dimensionless stiffness submatrices associated with the stationary and purely moving modes of the moving nanobeam are provided in Appendix B.

6.1.3. A comparison study

Consider a simply supported moving silver nanobeam whose length and radius in order are 50 nm and 4 nm. The predicted dimensionless divergence velocities pertinent to the first five modes by the proposed methodologies in Section 6.1.1 and 6.1.2 have been presented in Table 1. The divergence velocity of the ith flexural vibration mode is expressed by $v_{x_i}^d = \sqrt{\frac{E_b}{\rho_b}}\,\beta_i^d$. To apply the suggested numerical method, we set $NM = 10$ to all proposed models. A brief survey of the obtained results shows that there exists a reasonably good agreement between the predicted results by the AS and those of the NS for all suggested models. In the case of RBM, the predicted results by the AS are coincident with those of the NS. The main reason for this fact is that both dimensionless stiffness submatrices associated with the stationary and purely moving modes are

Table 1
Comparison of the predicted first five divergent velocities by the analytical approach and those of the AMM via the surface-energetic RBM, TBM, and HOBM.

Model	Method	β_1^d	β_2^d	β_3^d	β_4^d	β_5^d
RBM	AS[a]	0.16318502	0.30193315	0.42479675	0.52700037	0.60916885
	NS[b]	0.16318502	0.30193315	0.42479675	0.52700037	0.60916885
TBM	AS	0.15857566	0.27282791	0.35503531	0.41211002	0.45223247
	NS	0.15856484	0.27276725	0.35489504	0.41187989	0.45191375
HOBM	AS	0.15809812	0.27009140	0.34965465	0.40498016	0.44463583
	NS	0.15834401	0.27137381	0.35228927	0.39908384	0.40856257

[a]Analytical solution.
[b]Numerical solution.

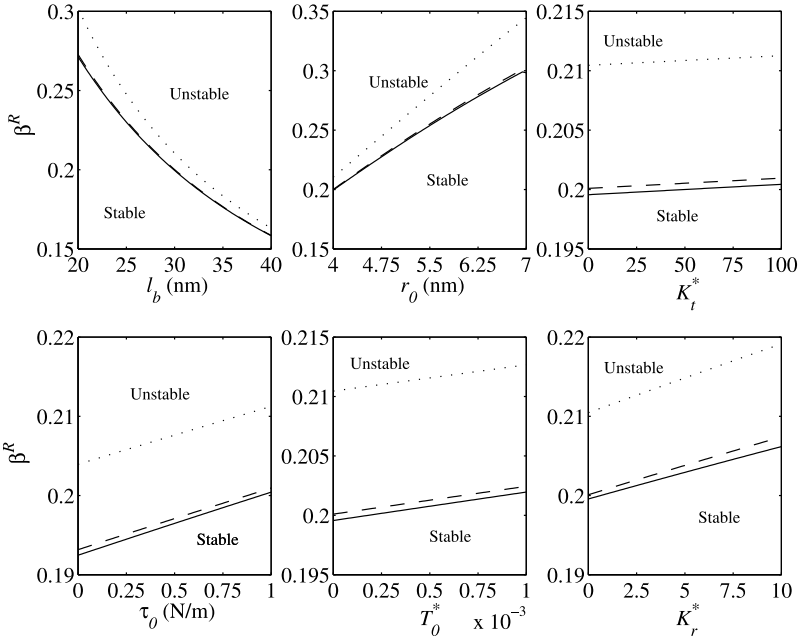

Fig. 2. Variation of the critical divergence velocity in terms of: (a) NW's length, (b) NW's radius, (c) dimensionless transverse stiffness, (d) residual surface stress, (e) dimensionless pretensioning force, (f) dimensionless rotational stiffness; ($l_b = 20$ nm, $r_0 = 4$ nm, $K_t^* = K_t l_{b0}^4/(E_b I_b)$, $T_0^* = T_0/(E_b A_b)$, $K_r^* = K_r l_{b0}^2/(E_b I_b)$, $l_{b0} = 100$ nm, (...) RBM, (− − −) TBM, (−) HOBM).

diagonal. For the moving nanostructure modeled based on the TBM and HOBM, the relative discrepancies between the divergence velocities by the AS and those of the NS would grow as the mode number increases. Such relative discrepancies are limited to 0.07 and 8.8 percent for the TBM and HOBM, respectively.

6.1.4. Influential factors on stability of moving nanobeams

Fig. 2(a)–(f) display the plots of dimensionless critical divergence velocity as a function of nanobeam's length, nanobeam's radius, residual surface stress, pretensioning force, and transverse and rotational stiffness of the surrounding medium. The plots pertinent to the RBM, TBM, and HOBM are specified by dotted, dashed, and solid lines, respectively. As it is obvious from the demonstrated results, all proposed models predict that the critical divergence velocity of the moving nanobeam would reduce by increasing the nanobeam's length. However, an increase of the nanobeam's radius, transverse or rotational stiffness of the surrounding elastic medium, pretensioning force, or residual surface stress (with a positive sign) would lead to growing of the critical divergence velocity; thereby, the stability of the moving nanostructure would increase by growing such parameters. Concerning the role of the shear deformation on the divergence velocity, the obtained results show that the predicted critical divergence velocities by the TBM and HOBM are lower than those obtained by the RBM since the flexural stiffness of the moving nanobeam by the RBM is commonly overestimated due to not considering the shear strain energy in its formulations. A close scrutiny of the plotted results reveals that the relative discrepancies between the predicted divergence velocity by the RBM and those of the TBM or HOBM would lessen as the nanobeam's length, residual surface stress, pretensioning force, or transverse stiffness of the surrounding medium increases. Nevertheless, such discrepancies would magnify as nanobeam's radius or rotational stiffness of the surrounding medium increases. Another interesting investigation

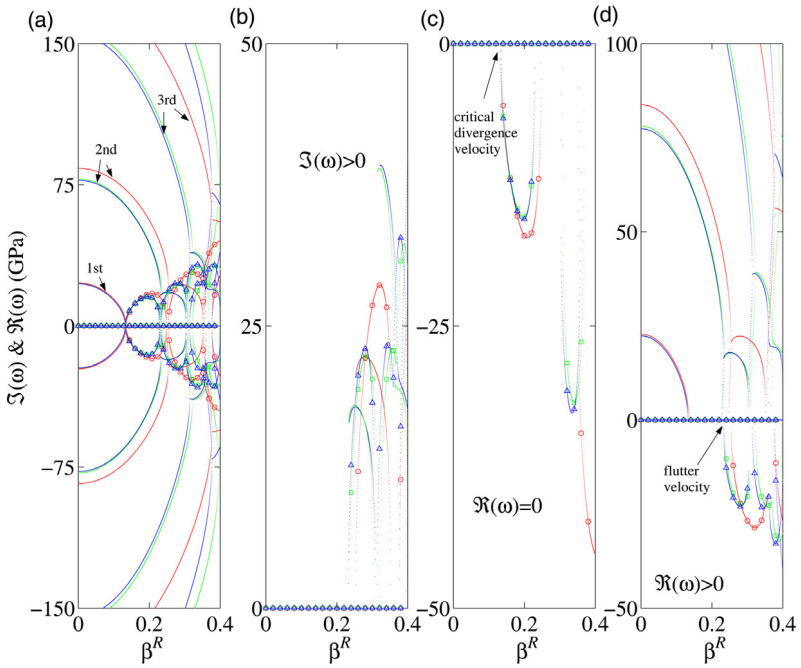

Fig. 3. Plots of flexural frequencies of an axially moving nanoscaled beam as a function of the dimensionless velocity for RBM, TBM, and HOBM: (a) ω-β^R, (b) $\Im(\omega) > 0$, (c) $\Re(\omega) = 0$, (d) $\Re(\omega) > 0$; ((···) RBM, (···) TBM, (···) HOBM; $l_b = 50$ nm, $D_0 = 8$ nm, $NM = 6$) . (For interpretation of the references to color in this figure legend, the reader is referred to the web version of this article.)

is to determine the stable and unstable regions under various conditions. As it is seen in Fig. 2(a)–(f), the regions under the plotted results present dynamically stable zones. In other words, the moving nanobeam would be surely stable for velocities lower than the critical divergence velocity. However, for velocities higher than the critical one, the moving nanostructure would be unstable. Actually, for such velocities, any cause of lateral motion would result in large dynamic deflections and stresses within the nanostructure. The suggested theories could not display these critical phenomena in the context of small deflections.

As it will be displayed in the upcoming parts, it cannot be exactly mentioned that the moving nanobeam would be unstable for all velocities beyond the critical divergence velocities. In fact, there also exist small velocity intervals (i.e., for velocities between that of the end of divergence instability zone and the flutter velocity) at which the supersonic moving nanostructure would be stable.

6.2. More details on free dynamic response of moving nanobeams

The transverse vibrations of moving nanobeams are highly influenced by the signs of the imaginary part and real part of the flexural frequencies (i.e., $\Im(\omega)$ and $\Re(\omega)$). Generally, for the nonzero real part, three cases would occur: (i) the imaginary part is zero: the moving nanostructure would be stable and it vibrates harmonically; (ii) the imaginary part is negative: flutter instability takes place and the amplitudes of dynamic deflections would grow exponentially as the time goes by; (iii) the imaginary part is positive: the moving nanostructure would be stable, and any dynamic deformation is damped with time. For frequencies whose real part is zero, two cases are possible: (i) the imaginary part is negative: the moving nanobeam arrives at divergence instability; (ii) the imaginary part is positive: any cause of deformation within the moving nanobeam would decrease exponentially as time passes, and thereby, the nanostructure would be stable. In the following parts, the real and imaginary parts of the flexural frequencies that correspond to the dominant vibration modes are extracted and plotted in terms of velocity according to the RBM, TBM, and HOBM.

In Fig. 3(a), the plots of real and imaginary parts of the flexural frequencies of the axially moving nanobeam in terms of dimensionless velocity have been provided for the suggested models. The real part of frequencies of the RBM, TBM, and HOBM has been specified by the dotted black, green, and blue colors, respectively, while their imaginary parts in order have been provided with the same color by the dotted circle, dotted square, and dotted triangle signs. For more convenience in dynamic analysis of the moving nanostructure, the plots of frequencies with positive imaginary part have been extracted from those in Fig. 3(a) and re-plotted as a function of dimensionless velocity in Fig. 3(b). These plots present the imaginary part of flexural frequencies of dynamically stable modes. It should be noted that the moving nanobeam would be stable for a given velocity if its stability would not be endangered in all vibration modes for that velocity. In this regard, the plots of the imaginary part of frequencies when their real parts are zero, as well as the plots of real and imaginary parts of frequencies with positive

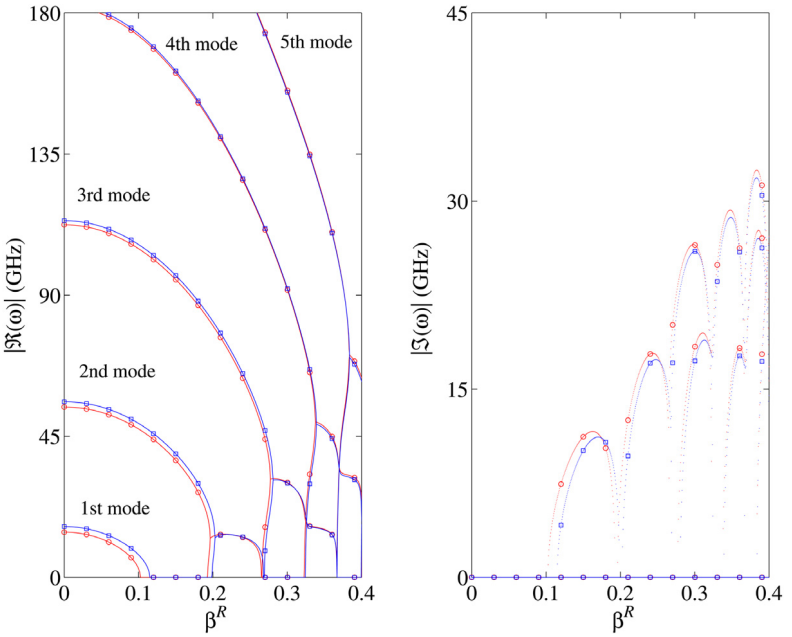

Fig. 4. Plots of real and imaginary parts of the predicted flexural frequencies by the HOBM as a function of the dimensionless velocity with and without considering the surface effect; ((.. ○ ..) CET, (..□..) SET; $l_b = 60$ nm, $D_0 = 8$ nm, $NM = 8$, $T_0 = K_t = K_r = 0$).

real parts and negative imaginary parts, have been demonstrated in Fig. 3(c) and (d). Actually, the plotted results in Fig. 3(c) show the divergence modes on the basis of the RBM, TBM, and HOBM. As it obvious, the critical divergence velocities of the moving nanobeam accounting for the surface effect in order are $0.135\sqrt{E_b/\rho_b}$, $0.132\sqrt{E_b/\rho_b}$, and $0.131\sqrt{E_b/\rho_b}$ using the RBM, TBM, and HOBM. Further, a close scrutiny of the demonstrated results indicates that the RBM, TBM, and HOBM predict that the first and the second divergence velocity intervals would be ([0.135,0.248]$\sqrt{E_b/\rho_b}$,[0.351,0.446]$\sqrt{E_b/\rho_b}$), ([0.132,0.231]$\sqrt{E_b/\rho_b}$,[0.308,0.368]$\sqrt{E_b/\rho_b}$), and ([0.131,0.228]$\sqrt{E_b/\rho_b}$,[0.303,0.360]$\sqrt{E_b/\rho_b}$), respectively. In Fig. 3(d), the plots with negative value for the imaginary parts of the flexural frequencies represent the flutter modes. For such frequencies, any small lateral deflection yields large dynamic deflection and if such a deflection could not be appropriately damped, this matter would result in high stresses which lead to the collapse of the moving nanostructure. According to the RBM, TBM, and HOBM, the critical flutter velocities in order are approximately equal to $0.254\sqrt{E_b/\rho_b}$, $0.235\sqrt{E_b/\rho_b}$, and $0.233\sqrt{E_b/\rho_b}$. Additionally, the first two velocity intervals associated with the flutter instability via the RBM, TBM, and HOBM are identified as: ([0.254,0.351]$\sqrt{E_b/\rho_b}$,[0.377,0.446]$\sqrt{E_b/\rho_b}$), ([0.235,0.308]$\sqrt{E_b/\rho_b}$,[0.322,0.368]$\sqrt{E_b/\rho_b}$), and ([0.233,0.304]$\sqrt{E_b/\rho_b}$,[0.312,0.360]$\sqrt{E_b/\rho_b}$), respectively. As it is seen, the predicted results by the TBM are close to those of the HOBM since these two theories include shear strain energy in evaluation of transverse stiffness of the moving nanostructure. Due to this fact, the predicted divergence and flutter velocities by the TBM and HOBM are commonly lower than those of the RBM. It implies that the RBM overestimates both divergence and flutter velocities with respect to the TBM and HOBM.

6.3. Influence of the surface energy

A pivotal study is performed to investigate the influence of the surface effect on the free dynamic response of the moving nanobeam. For this purpose, the predicted first five flexural frequencies by the HOBM for a moving nanobeam with $l_b = 60$ nm and $D_0 = 8$ nm have been plotted in Fig. 4. The results have been demonstrated for two cases: with and without consideration of the surface energy whose results in order are identified by the dotted-square markers and dotted-circle markers. For a particular value of the velocity, the predicted flexural frequencies (i.e., the real part) would increase by considering the surface effect. It is mainly related to the positive incorporation of both residual surface stress and surface elastic modulus (i.e., τ_0 and $\lambda_0 + 2\mu_0$) of the silver nanobeam [001] into the transverse stiffness according to the proposed surface energetic models. As it is obvious, the influence of the surface energy on the variation of the fundamental frequency is more apparent with respect to that of other vibration modes. Actually, as the mode number increases, the effect of surface energy on the free vibration behavior of the nanostructure would reduce. Furthermore, by increasing the velocity of the moving nanobeam, the role of the velocity on the fundamental frequency becomes highlighted such that the maximum influence is observed at the critical divergence velocity. This matter is mainly ascertained to the very low level of the transverse stiffness of the traveling nanobeam at velocities near to the divergence speeds. In such circumstances, any cause of strengthening the lateral stiffness like the surface effect would result in a significant impact on the free dynamic response of the moving nanobeam.

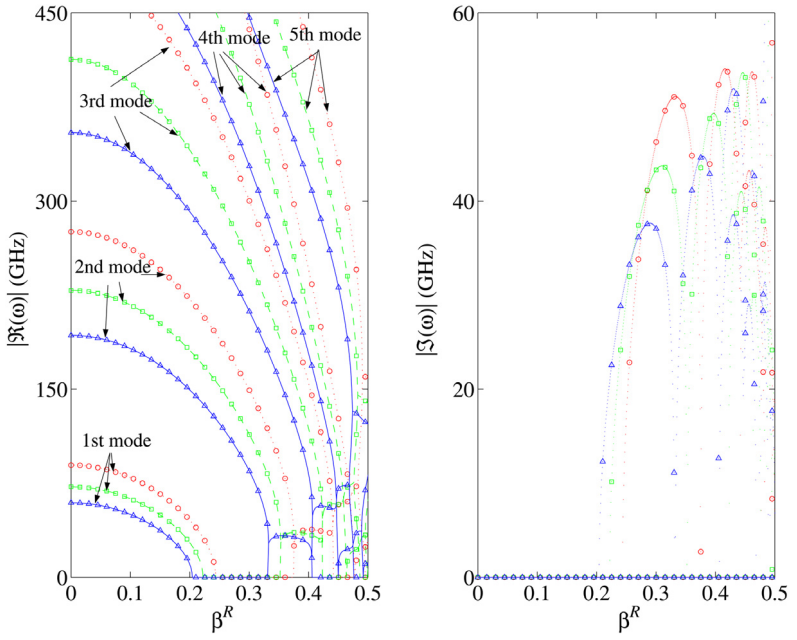

Fig. 5. Plots of real and imaginary parts of the predicted flexural frequencies by the HOBM as a function of dimensionless velocity for different levels of the nanobeam's length; ((.. ○ ..) $l_b = 23$ nm, (.. □ ..) $l_b = 26$ nm, (.. △ ..) $l_b = 29$ nm; $D_0 = 8$ nm, $NM = 8$, $T_0 = K_t = K_r = 0$).

Concerning the effect of the surface energy on the instability of the moving nanobeam, the plotted imaginary part of flexural frequencies as a function of dimensionless velocity reveals that the divergence instability would be initiated as the axial velocity reaches $0.102\sqrt{E_b/\rho_b}$ and $0.115\sqrt{E_b/\rho_b}$ based on the classical elasticity theory (CET) and the surface elasticity theory (SET), respectively. Further, the proposed HOBM predicts that the moving nanobeam would be dynamically unstable for velocities within the intervals $[0.102, 0.193]\sqrt{E_b/\rho_b}$ and $[0.115, 0.199]\sqrt{E_b/\rho_b}$ on the basis of the CET and the SET, respectively. In fact, these represent the first divergence interval of velocities with and without considering the surface effect. Thereafter, a close scrutiny of the plotted results indicates that the moving nanobeam would be dynamically stable at a very narrow interval of velocities $[0.193, 0.196]\sqrt{E_b/\rho_b}$ and $[0.199, 0.203]\sqrt{E_b/\rho_b}$ using the CET and SET, respectively. By passing the first flutter velocities (i.e., $0.196\sqrt{E_b/\rho_b}$, $0.203\sqrt{E_b/\rho_b}$), the flutter instability occurs, and the moving nanobeam would not be stable any more and any cause of lateral motion will develop large deflections and stresses within the moving nanobeam until it would collapse. More investigations reveal that as long as the velocity of the moving nanobeam would be in the ranges of $[0.196, 0.265]\sqrt{E_b/\rho_b}$ and $[0.203, 0.2685]\sqrt{E_b/\rho_b}$, in order on the basis of the CET and SET, the flutter instability could take place. Additionally, the corresponding velocities to the onset of the second divergence instability (i.e., second divergence velocities) are $0.2665\sqrt{E_b/\rho_b}$ via the CET-based HOBM and $0.2695\sqrt{E_b/\rho_b}$ via the SET-based HOBM, and the second flutter velocities associated with these models in order are $0.277\sqrt{E_b/\rho_b}$ and $0.2805\sqrt{E_b/\rho_b}$. All these numerical examples prove that the surface energy would help the stability of the moving silver nanobeam.

6.4. Influence of the length of nanobeams

Determination of the role of the nanobeam's length on its free vibration behavior is also of high interest. Using surface energy-based HOBM, the predicted first five frequencies of the moving nanobeam as a function of velocity have been demonstrated in Fig. 5 for three levels of the nanobeam's length (i.e., $l_b = 23$, 26, and 29 nm). The plotted results are given for the case of $D_0 = 8$ nm and $T_0 = K_t = K_r = 0$. Irrespective of the velocity level of the moving nanobeam, the frequencies would reduce by increasing the length of the nanobeam. Such a reduction is more apparent at the velocities close to the critical divergence velocity. For all considered values of the nanobeam's length, an increase of the axial velocity leads to a reduction of flexural frequencies of the moving nanobeam. Again, the variation of the velocity in the neighborhood of the critical divergence velocity has the most influence on the variation of the flexural frequencies.

As it is obvious from the plotted results, the critical divergence velocity would reduce by growing the length of the moving nanobeam. For example, the velocity intervals associated with the divergence instability for $l_b = 23$, 26, and 29 nm in order are $[0.243, 0.375]\sqrt{E_b/\rho_b}$, $[0.222, 0.352]\sqrt{E_b/\rho_b}$, and $[0.204, 0.331]\sqrt{E_b/\rho_b}$. The first flutter velocities of these lengths are approximately equal to $0.3753\sqrt{E_b/\rho_b}$, $0.3529\sqrt{E_b/\rho_b}$, and $0.3325\sqrt{E_b/\rho_b}$, respectively. Thereby, for nanobeams with $l_b = 23$, 26, and 29 nm, the axially moving nanostructure would be dynamically stable for velocities in the intervals $[0.375, 0.3753]\sqrt{E_b/\rho_b}$, $[0.352, 0.3529]\sqrt{E_b/\rho_b}$, and $[0.331, 0.3325]\sqrt{E_b/\rho_b}$. As it is obvious, the bandwidth of such stable velocity intervals would reduce as the length of the nanobeam decreases. The obtained results confirm this fact that both divergence and flutter velocities would reduce by increasing the nanobeam's length.

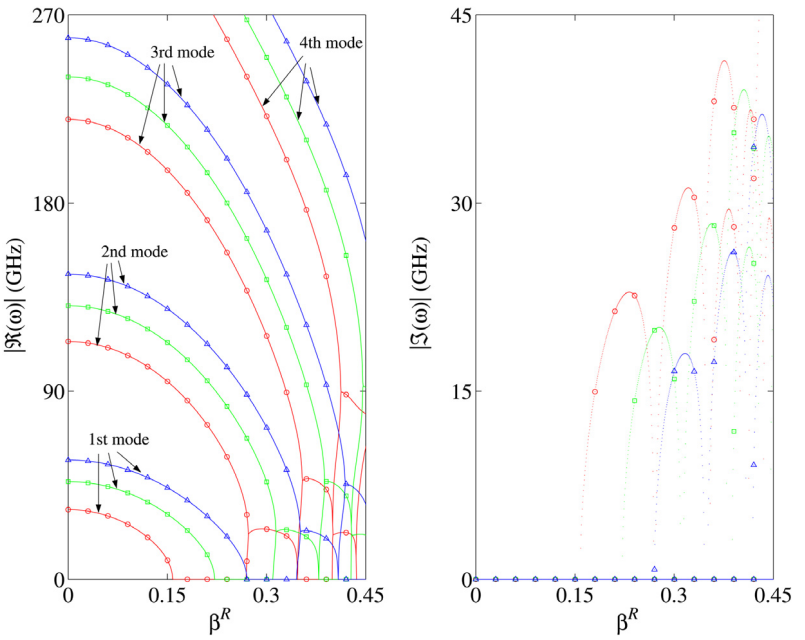

Fig. 6. Plots of real and imaginary parts of the predicted flexural frequencies by the HOBM as a function of the dimensionless velocity for various values of pretensioning force; ((.. ○ ..) $\overline{T}_0^R = 0$, (.. □ ..) $\overline{T}_0^R = 10$, (.. △ ..) $\overline{T}_0^R = 20$; $l_b = 40$ nm, $D_0 = 8$ nm, $NM = 6$, $K_t = K_r = 0$).

6.5. Influence of the pretensioning force

We are also interested in the role of pretensioning force on the free dynamic response of the moving nanobeam. To this end, the plotted results of absolute values of real and imaginary parts of the first four flexural frequencies as a function of dimensionless velocity have been provided for three levels of the pretensioning force (i.e., $\overline{T}_0^R = 0$, 10, and 20). The results have been extracted using HOBM for a fairly stocky nanobeam with $l_b = 40$ nm and $D_0 = 8$ nm. As it is evident from the demonstrated results, the flexural frequency of each vibration mode would increase as the pretensioning force increases. By increasing the velocity of the moving nanobeam up to the divergence one, the influence of the pretensioning force on the free dynamic response of the nanostructure becomes highlighted. It implies that at the velocities close to the divergence velocity, the variation of the pretensioning force has the most influence on the internal stiffness as well as the flexural frequencies of the moving nanobeam. Additionally, the role of pretensioning force on the frequencies would reduce as the mode number increases. In other words, the pretensioning force has the most impact on the fundamental frequency of the moving nanobeam. Generally, the variation of the velocity has more influence on the variation of flexural frequencies of the moving nanobeam acted upon by higher pretensioning forces. Further, the frequencies of higher modes are more affected by the variation of the velocity.

According to the plotted results in Fig. 6, the critical divergence velocity of the moving nanobeam would magnify by increasing of the pretensioning force; however, the corresponding bandwidth of the velocity intervals of the divergence zone would commonly reduce as the pretensioning force within the moving nanostructure increases. For instance, the velocity intervals pertinent to the moving nanobeam with $\overline{T}_0^R = 0$, 10, and 20 are $[0.157, 0.269]\sqrt{E_b/\rho_b}$, $[0.222, 0.311]\sqrt{E_b/\rho_b}$, and, $[0.270, 0.346]\sqrt{E_b/\rho_b}$, respectively. Additionally, the flutter velocities associated with these pretensioning forces in order are $0.272\sqrt{E_b/\rho_b}$, $0.314\sqrt{E_b/\rho_b}$, and $0.351\sqrt{E_b/\rho_b}$. In view of the given velocity intervals of divergence instability zone, it could be readily found that the moving nanobeam with $\overline{T}_0 = 0$, 10, and 20 would be dynamically stable when it moves with supersonic speeds in the narrow velocity intervals $[0.269, 0.272]\sqrt{E_b/\rho_b}$, $[0.311, 0.314]\sqrt{E_b/\rho_b}$, and, $[0.346, 0.351]\sqrt{E_b/\rho_b}$, respectively. This brief survey also reveals this fact that the bandwidth of the velocity intervals corresponds to stable traveling nanobeams after the divergence zones would commonly increase by growing of the pretensioning force.

7. Concluding remarks

Free vibrations and dynamic instability of axially moving nanobeams rested on an elastic bed were studied. In the framework of the surface elasticity theory of Gurtin–Murdoch, the equations of motion were derived on the basis of the RBM, TBM, and HOBM by employing Hamilton's principle. By exploiting the Galerkin-based AMM, the governing PDEs were reduced to appropriate ODEs for each model. The eigenvalue problems were then solved for natural frequencies under various levels of the nanobeam's velocity. The important unstable regions of the moving nanostructure, namely divergence

and flutter zones, were determined. Given the importance of the subject, the critical flexural and shear divergence velocities of various modes were obtained both analytically and numerically. The capabilities of the suggested approximate analytical method were checked by comparing its predicted results with those of the numerical approach, and a reasonably good agreement was reported. The influence of the nanobeam's length and diameter, lateral and rotational stiffness of the elastic bed, residual surface stress, shear strain energy, and pretensioning force on the divergence velocities was displayed and discussed. For a wide range of the velocity of the moving nanobeam, the roles of the surface energy, nanobeam's length, shear deformation, and pretensioning force on natural frequencies as well as divergence and flutter instability of the moving nanostructure were also examined.

Appendix A. The values of $a_m^{[.]}, b_m^{[.]}, c_m^{[.]}$; $[.] = T$ or H

$$a_m^T = \left(1+\chi_1^T\right)\left(1+\chi_2^T\right)\lambda^{-2}(m\pi)^4, \tag{A.1a}$$

$$\begin{aligned} b_m^T = {} & (m\pi)^2\left(1+\chi_1^T\right)\left(1+(m\pi)^2\left(\eta+\chi_5^T\right)+\overline{K}_r^T\right)+(m\pi)^2\lambda^{-2}\left(1+\chi_2^T\right)\times \\ & \left(\overline{K}_t^T+(m\pi)^2\left(1+\overline{T}_0^T+\chi_6^T\right)\right)-(m\pi)^4\chi_3^T\lambda^{-2}, \end{aligned} \tag{A.1b}$$

$$\begin{aligned} c_m^T = {} & \left(1+(m\pi)^2\left(\eta+\chi_5^T\right)+\overline{K}_r^T\right)\left(\overline{K}_t^T+(m\pi)^2\left(1+\overline{T}_0^T+\chi_6^T\right)\right) \\ & -(m\pi)^2\left(1+(m\pi)^2\chi_4^T\right), \end{aligned} \tag{A.1c}$$

$$\begin{aligned} a_m^H = {} & (m\pi)^2\left(\gamma_7^2+\gamma_8^2\left(1+\chi_4^H\right)(m\pi)^2+\overline{K}_r^H\right)\times \\ & \left(\left(1+\chi_5^H\right)-\gamma_2^2\left(1+\chi_{10}^H\right)(m\pi)^2\right)+(m\pi)^2\gamma_1^2\gamma_6^2\left(1+\chi_1^H\right)\left(1+\chi_2^H\right), \end{aligned} \tag{A.1d}$$

$$\begin{aligned} b_m^H = {} & (m\pi)^2\left(1+\chi_1^H\right)\left(\overline{K}_t^H+(m\pi)^4\left(1-\chi_7^H\right)+(m\pi)^2\left(\gamma_3^2+\overline{T}_0^H+\chi_6^H\right)\right) \\ & +(m\pi)^2\left(\overline{K}_r^H+(m\pi)^2\left(1+\chi_4^H\right)\gamma_8^2+\gamma_7^2\right)\left(\left(1+\chi_5^H\right)-(m\pi\gamma_2)^2\left(1+\chi_{10}^H\right)\right) \\ & -(m\pi)^4\gamma_6^2\left(1+\chi_1^H\right)\left(\left(1+\chi_8^H\right)\gamma_9^2(m\pi)^2-\gamma_3^2\right) \\ & -(m\pi)^4\gamma_1^2\left(1+\chi_1^H\right)\left(\gamma_7^2-(m\pi\gamma_9)^2\left(1+\chi_3^H\right)\right), \end{aligned} \tag{A.1e}$$

$$\begin{aligned} c_m^H = {} & \left(\overline{K}_r^H+(m\pi)^2\left(1+\chi_4^H\right)\gamma_8^2+\gamma_7^2\right)\times \\ & \left(\overline{K}_t^H+(m\pi)^4\left(1-\chi_7^H\right)+(m\pi)^2\left(\gamma_3^2+\overline{T}_0^H+\chi_6^H\right)\right) \\ & -(m\pi)^2\left(\gamma_7^2-(m\pi\gamma_9)^2\left(1+\chi_3^H\right)\right)\left(\gamma_3^2-(m\pi\gamma_4)^2\left(1+\chi_8^H\right)\right). \end{aligned} \tag{A.1f}$$

Appendix B. Stiffness submatrices pertinent to the stationary and purely moving modes of the moving nanobeam

$$\left[\overline{\mathbf{K}}_{bs}^R\right]_{ij}^{ww} = \int_0^1\left(\left(1+\chi_3^R\right)\frac{\mathrm{d}^2\phi_i^w}{\mathrm{d}\xi^2}\frac{\mathrm{d}^2\phi_j^w}{\mathrm{d}\xi^2}+\left(\chi_4^R+\overline{K}_r^R\right)\frac{\mathrm{d}\phi_i^w}{\mathrm{d}\xi}\frac{\mathrm{d}\phi_j^w}{\mathrm{d}\xi}+\overline{K}_t^R\phi_i^w\phi_j^w\right)\mathrm{d}\xi, \tag{B.1a}$$

$$\left[\overline{\mathbf{K}}_{bm}^R\right]_{ij}^{ww} = -\int_0^1\left(\lambda^2\left(1+\chi_1^R\right)\phi_i^w\frac{\mathrm{d}^2\phi_j^w}{\mathrm{d}\xi^2}-\left(1+\chi_2^R\right)\phi_i^w\frac{\mathrm{d}^4\phi_j^w}{\mathrm{d}\xi^4}\right)\mathrm{d}\xi, \tag{B.1b}$$

$$\left[\overline{\mathbf{K}}_{bs}^T\right]_{ij}^{\theta\theta} = \int_0^1\left(\left(1+\overline{K}_r^T\right)\phi_i^\theta\phi_j^\theta+\left(\eta+\chi_5^T\right)\frac{\mathrm{d}\phi_i^\theta}{\mathrm{d}\xi}\frac{\mathrm{d}\phi_j^\theta}{\mathrm{d}\xi}\right)\mathrm{d}\xi, \tag{B.1c}$$

$$\left[\overline{\mathbf{K}}_{bs}^T\right]_{ij}^{\theta w} = -\int_0^1\left(\phi_i^\theta\frac{\mathrm{d}\phi_j^w}{\mathrm{d}\xi}+\chi_4^T\frac{\mathrm{d}\phi_i^\theta}{\mathrm{d}\xi}\frac{\mathrm{d}^2\phi_j^w}{\mathrm{d}\xi^2}\right)\mathrm{d}\xi, \tag{B.1d}$$

$$\left[\overline{\mathbf{K}}_{bs}^T\right]_{ij}^{w\theta} = -\int_0^1\frac{\mathrm{d}\phi_i^w}{\mathrm{d}\xi}\phi_j^\theta\,\mathrm{d}\xi, \tag{B.1e}$$

$$\left[\overline{\mathbf{K}}_{bs}^{T}\right]_{ij}^{ww} = \int_0^1 \left(\left(1+\chi_6^T+\overline{T}_0^T\right) \frac{\mathrm{d}\phi_i^w}{\mathrm{d}\xi}\frac{\mathrm{d}\phi_j^w}{\mathrm{d}\xi} + \overline{K}_t^T \phi_i^w \phi_j^w \right) \mathrm{d}\xi, \tag{B.1f}$$

$$\left[\overline{\mathbf{K}}_{bm}^{T}\right]_{ij}^{\theta\theta} = -\int_0^1 \lambda^{-2} \left(1+\chi_2^T\right) \phi_i^\theta \frac{\mathrm{d}^2\phi_j}{\mathrm{d}\xi^2}\,\mathrm{d}\xi, \tag{B.1g}$$

$$\left[\overline{\mathbf{K}}_{bm}^{T}\right]_{ij}^{\theta w} = -\int_0^1 \chi_3^T \lambda^{-2} \frac{\mathrm{d}^3\phi_i^\theta}{\mathrm{d}\xi^3}\phi_j^w\,\mathrm{d}\xi, \tag{B.1h}$$

$$\left[\overline{\mathbf{K}}_{bm}^{T}\right]_{ij}^{ww} = -\int_0^1 \left(1+\chi_1^T\right) \phi_i^w \frac{\mathrm{d}^2\phi_j^w}{\mathrm{d}\xi^2}\,\mathrm{d}\xi, \tag{B.1i}$$

$$\left[\overline{\mathbf{K}}_{bs}^{H}\right]_{ij}^{\psi\psi} = \int_0^1 \left(\left(\overline{K}_r^H+\gamma_7^2\right)\phi_i^\psi\phi_j^\psi + \gamma_8^2\left(1+\chi_4^H\right)\frac{\mathrm{d}\phi_i^\psi}{\mathrm{d}\xi}\frac{\mathrm{d}\phi_j^\psi}{\mathrm{d}\xi} \right)\mathrm{d}\xi, \tag{B.1j}$$

$$\left[\overline{\mathbf{K}}_{bs}^{H}\right]_{ij}^{\psi w} = -\int_0^1 \left(\gamma_7^2\phi_i^\psi\frac{\mathrm{d}\phi_j^w}{\mathrm{d}\xi} - \gamma_9^2\left(1+\chi_3^H\right)\frac{\mathrm{d}\phi_i^\psi}{\mathrm{d}\xi}\frac{\mathrm{d}^2\phi_j^w}{\mathrm{d}\xi^2} \right)\mathrm{d}\xi, \tag{B.1k}$$

$$\left[\overline{\mathbf{K}}_{bs}^{H}\right]_{ij}^{w\psi} = -\int_0^1 \left(\gamma_3^2\frac{\mathrm{d}\phi_i^w}{\mathrm{d}\xi}\phi_j^\psi - \gamma_4^2\frac{\mathrm{d}^2\phi_i^w}{\mathrm{d}\xi^2}\frac{\mathrm{d}\phi_j^\psi}{\mathrm{d}\xi} \right)\mathrm{d}\xi, \tag{B.1l}$$

$$\left[\overline{\mathbf{K}}_{bs}^{H}\right]_{ij}^{ww} = \int_0^1 \left(\left(\gamma_3^2+\chi_6^H+\overline{T}_0^H\right)\frac{\mathrm{d}\phi_i^w}{\mathrm{d}\xi}\frac{\mathrm{d}\phi_j^w}{\mathrm{d}\xi} + \left(1-\chi_7^H\right)\frac{\mathrm{d}^2\phi_i^w}{\mathrm{d}\xi^2}\frac{\mathrm{d}^2\phi_j^w}{\mathrm{d}\xi^2} + \overline{K}_t^H\phi_i^w\phi_j^w \right)\mathrm{d}\xi, \tag{B.1m}$$

$$\left[\overline{\mathbf{K}}_{bm}^{H}\right]_{ij}^{\psi\psi} = -\int_0^1 \left(1+\chi_1^H\right)\phi_i^\psi\frac{\mathrm{d}^2\phi_j^\psi}{\mathrm{d}\xi^2}\,\mathrm{d}\xi, \tag{B.1n}$$

$$\left[\overline{\mathbf{K}}_{bm}^{H}\right]_{ij}^{\psi w} = -\int_0^1 \gamma_6^2\left(1+\chi_2^H\right)\phi_i^\psi\frac{\mathrm{d}^3\phi_j^w}{\mathrm{d}\xi^3}\,\mathrm{d}\xi, \tag{B.1o}$$

$$\left[\overline{\mathbf{K}}_{bm}^{H}\right]_{ij}^{w\psi} = -\int_0^1 \gamma_1^2\frac{\mathrm{d}\phi_i^w}{\mathrm{d}\xi}\frac{\mathrm{d}^2\phi_j^\psi}{\mathrm{d}\xi^2}\,\mathrm{d}\xi, \tag{B.1p}$$

$$\left[\overline{\mathbf{K}}_{bm}^{H}\right]_{ij}^{ww} = -\int_0^1 \left(\left(1+\chi_5^H\right)\phi_i^w\frac{\mathrm{d}^2\phi_j^w}{\mathrm{d}\xi^2} + \gamma_2^2\frac{\mathrm{d}\phi_i^w}{\mathrm{d}\xi}\frac{\mathrm{d}^3\phi_j^w}{\mathrm{d}\xi^3} \right)\mathrm{d}\xi. \tag{B.1q}$$

References

[1] M. Law, L.E. Greene, J.C. Johnson, R. Saykally, P. Yang, Nanowire dye-sensitized solar cells, Nature Mater. 4 (6) (2005) 455–459.
[2] B. Tian, X. Zheng, T.J. Kempa, Y. Fang, N. Yu, G. Yu, J. Huang, C.M. Lieber, Coaxial silicon nanowires as solar cells and nanoelectronic power sources, Nature 449 (7164) (2007) 885–889.
[3] E. Garnett, P. Yang, Light trapping in silicon nanowire solar cells, Nano Lett. 10 (3) (2010) 1082–1087.
[4] L.F. Cui, Y. Yang, C.M. Hsu, Y. Cui, Carbon-silicon core–shell nanowires as high capacity electrode for lithium ion batteries, Nano Lett. 9 (9) (2009) 3370–3374.
[5] M.S. Park, G.X. Wang, Y.M. Kang, D. Wexler, S.X. Dou, H.K. Liu, Preparation and electrochemical properties of SnO_2 nanowires for application in lithium-ion batteries, Angew. Chem.-Ger. Edit. 119 (5) (2007) 764–767.
[6] F. Patolsky, B.P. Timko, G.F. Zheng, C.M. Lieber, Nanowire-based nanoelectronic devices in the life sciences, MRS Bull. 32 (02) (2007) 142–149.
[7] Y. Li, F. Qian, J. Xiang, C.M. Lieber, Nanowire electronic and optoelectronic devices, Mater. Today 9 (10) (2006) 18–27.
[8] N.A. Melosh, A. Boukai, F. Diana, B. Gerardot, A. Badolato, P.M. Petroff, J.R. Heath, Ultrahigh-density nanowire lattices and circuits, Science 300 (5616) (2003) 112–115.
[9] R.S. Friedman, M.C. McAlpine, D.S. Ricketts, D. Ham, C.M. Lieber, Nanotechnology: high-speed integrated nanowire circuits, Nature 434 (7037) (2005) 1085–1085.
[10] Y. Cui, Z. Zhong, D. Wang, W.U. Wang, C.M. Lieber, High performance silicon nanowire field effect transistors, Nano Lett. 3 (2) (2003) 149–152.
[11] J. Goldberger, A.I. Hochbaum, R. Fan, P. Yang, Silicon vertically integrated nanowire field effect transistors, Nano Lett. 6 (5) (2006) 973–977.
[12] M.E. Gurtin, A.I. Murdoch, A continuum theory of elastic material surfaces, Arch. Ration. Mech. Anal. 57 (1975) 291–323.

[13] M.E. Gurtin, A.I. Murdoch, Effect of surface stress on wave propagation in solids, J. Appl. Phys. 47 (1976) 4414–4421.
[14] M.E. Gurtin, A.I. Murdoch, Surface stress in solids, Int. J. Solids Struct. 14 (1978) 431–440.
[15] R.E. Miller, V.B. Shenoy, Size-dependent elastic properties of nanosized structural elements, Nanotechnology 11 (3) (2000) 139.
[16] V.B. Shenoy, Atomistic calculations of elastic properties of metallic fcc crystal surfaces, Phys. Rev. B 71 (9) (2005) 094104.
[17] AC. Eringen, Nonlocal polar elastic continua, Int. J. Eng. Sci. 10 (1) (1972) 1–16.
[18] AC. Eringen, Nonlocal Continuum Field Theories, Springer Science & Business Media, 2002.
[19] J.N. Reddy, Nonlocal nonlinear formulations for bending of classical and shear deformation theories of beams and plates, Internat. J. Engrg. Sci. 48 (11) (2010) 1507–1518.
[20] R. Barretta, F.M. de Sciarra, A nonlocal model for carbon nanotubes under axial loads, Adv. Mater. Sci. Eng. 360935 (1–6) (2013).
[21] M. Canadija, R. Barretta, F.M. de Sciarra, On functionally graded Timoshenko nonisothermal nanobeams, Compos. Struct. 135 (2016) 286–296.
[22] F.M. de Sciarra, A general theory for nonlocal softening plasticity of integral-type, Int. J. Plast. 24 (8) (2008) 1411–1439.
[23] F.M. de Sciarra, Variational formulations and a consistent finite-element procedure for a class of nonlocal elastic continua, Int. J. Solids Struct. 45 (14–15) (2008) 4184–4202.
[24] K. Kiani, Nonlocal-integro-differential modeling of vibration of elastically supported nanorods, Physica E 83 (2016) 151–163.
[25] K. Kiani, Free dynamic analysis of functionally graded tapered nanorods via a newly developed nonlocal surface energy-based integro-differential model, Compos. Struct. 139 (2016) 151–166.
[26] G. Romano, R. Barretta, Nonlocal elasticity in nanobeams: the stress-driven integral model, Internat. J. Engrg. Sci. 115 (2017) 14–27.
[27] R. Barretta, M. Diaco, L. Feo, R. Luciano, F.M. de Sciarra, R. Penna, Stress-driven integral elastic theory for torsion of nano-beams, Mech. Res. Commun. 87 (2018) 35–41.
[28] L.Y. Jiang, Z. Yan, Timoshenko beam model for static bending of nanowires with surface effects, Physica E 42 (9) (2010) 2274–2279.
[29] J.L. Liu, Y. Mei, R. Xia, W.L. Zhu, Large displacement of a static bending nanowire with surface effects, Physica E 44 (10) (2012) 2050–2055.
[30] F.F. Mahmoud, M.A. Eltaher, A.E. Alshorbagy, E.I. Meletis, Static analysis of nanobeams including surface effects by nonlocal finite element, J. Mech. Sci. Technol. 26 (11) (2012) 3555–3563.
[31] D.M. Zhao, J.L. Liu, J. Sun, R.N. Wu, R. Xia, A revisit of internal force diagrams on nanobeams with surface effects, Curr. Nanosci. 11 (3) (2015) 388–393.
[32] G.F. Wang, X.Q. Feng, Timoshenko beam model for buckling and vibration of nanowires with surface effects, J. Phys. D Appl. Phys. 42 (15) (2009) 155411.
[33] Z. Yan, L.Y. Jiang, The vibrational and buckling behaviors of piezoelectric nanobeams with surface effects, Nanotechnology 22 (24) (2011) 245703.
[34] M.A. Eltaher, F.F. Mahmoud, A.E. Assie, E.I. Meletis, Coupling effects of nonlocal and surface energy on vibration analysis of nanobeams, Appl. Math. Comput. 224 (2013) 760–774.
[35] O. Rahmani, O. Pedram, Analysis and modeling the size effect on vibration of functionally graded nanobeams based on nonlocal Timoshenko beam theory, Internat. J. Engrg. Sci. 77 (2014) 55–70.
[36] K. Kiani, Surface effect on free transverse vibrations and dynamic instability of current-carrying nanowires in the presence of a longitudinal magnetic field, Phys. Lett. A 378 (26) (2014) 1834–1840.
[37] X.F. Li, J. Zou, S.N. Jiang, K.Y. Lee, Resonant frequency and flutter instability of a nanocantilever with the surface effects, Compos. Struct. 153 (2016) 645–653.
[38] K. Kiani, Dynamic interactions between double current-carrying nanowires in the presence of a longitudinal magnetic field: novel integro-surface energy-based models, Internat. J. Engrg. Sci. 107 (2016) 98–133.
[39] K. Kiani, Thermo-elasto-dynamic analysis of axially functionally graded non-uniform nanobeams with surface energy, Internat. J. Engrg. Sci. 106 (2016) 57–76.
[40] B. Gheshlaghi, S.M. Hasheminejad, Surface effects on nonlinear free vibration of nanobeams, Compos. Part B Eng. 42 (4) (2011) 934–937.
[41] P. Malekzadeh, M. Shojaee, Surface and nonlocal effects on the nonlinear free vibration of non-uniform nanobeams, Compos. Part B-Eng. 52 (2013) 84–92.
[42] P.A. Sharabiani, M.R.H. Yazdi, Nonlinear free vibrations of functionally graded nanobeams with surface effects, Compos. Part B-Eng. 45 (1) (2013) 581–586.
[43] S. Sahmani, M. Bahrami, M.M. Aghdam, R. Ansari, Surface effects on the nonlinear forced vibration response of third-order shear deformable nanobeams, Compos. Struct. 118 (2014) 149–158.
[44] S. Sahmani, M.M. Aghdam, M. Bahrami, On the free vibration characteristics of postbuckled third-order shear deformable FGM nanobeams including surface effects, Compos. Struct. 121 (2015) 377–385.
[45] D. Zhao, J. Liu, L. Wang, Nonlinear free vibration of a cantilever nanobeam with surface effects: semi-analytical solutions, Int. J. Mech. Sci. 113 (2016) 184–195.
[46] G.F. Wang, X.Q. Feng, Surface effects on buckling of nanowires under uniaxial compression, Appl. Phys. Lett. 94 (14) (2009) 141913.
[47] Z. Yan, L. Jiang, Surface effects on the electromechanical coupling and bending behaviours of piezoelectric nanowires, J. Phys. D Appl. Phys. 44 (7) (2011) 075404.
[48] K. Kiani, Column buckling analysis of a system of doubly parallel slender nanowires carrying electric current in a longitudinal magnetic field, J. Phys. Chem. Solids 95 (2016) 89–97.
[49] K. Kiani, Elastic buckling of current-carrying double-nanowire-systems immersed in a magnetic field, Acta Mech. 227 (12) (2016) 3549–3570.
[50] Y. Li, J. Song, B. Fang, J. Zhang, Surface effects on the postbuckling of nanowires, J. Phys. D Appl. Phys. 44 (42) (2011) 425304.
[51] R. Ansari, V. Mohammadi, M. Faghih Shojaei, R. Gholami, S. Sahmani, Postbuckling analysis of timoshenko nanobeams including surface stress effect, Internat. J. Engrg. Sci. 75 (2014) 1–10.
[52] K. Kiani, Exact postbuckling analysis of highly stretchable-surface energetic-elastic nanowires with various ends' conditions, Int. J. Mech. Sci. (2017) 124–125, 242–252.
[53] B. Tabarrok, C.M. Leech, Y.I. Kim, On the dynamics of an axially moving beam, J. Franklin Inst. 297 (3) (1974) 201–220.
[54] J.A. Wickert, C.D. Mote Jr., Classical vibration analysis of axially moving continua, ASME J. Appl. Mech. 57 (3) (1990) 738–744.
[55] J.A. Wickert, Non-linear vibration of a traveling tensioned beam, Int. J. Non-Linear Mech. 27 (3) (1992) 503–517.
[56] S.J. Hwang, N.C. Perkins, Supercritical stability of an axially moving beam part I: model and equilibrium analysis, J. Sound Vib. 154 (3) (1992) 381–396.
[57] H.R. Oz, M. Pakdemirli, Vibrations of an axially moving beam with time-dependent velocity, J. Sound Vib. 227 (2) (1999) 239–257.
[58] E. Ozkaya, M. Pakdemirli, Vibrations of an axially accelerating beam with small flexural stiffness, J. Sound Vib. 234 (3) (2000) 521–535.
[59] F. Vestroni, Nonlinear dynamics and bifurcations of an axially moving beam, J. Vib. Acoust. 122 (2000) 21.
[60] H.R. Oz, M. Pakdemirli, H. Boyaci, Non-linear vibrations and stability of an axially moving beam with time-dependent velocity, Int. J. NonLinear Mech. 36 (1) (2001) 107–115.
[61] F. Pellicano, F. Vestroni, Complex dynamics of high-speed axially moving systems, J. Sound Vib. 258 (1) (2002) 31–44.
[62] L.Q. Chen, X.D. Yang, Vibration and stability of an axially moving viscoelastic beam with hybrid supports, Eur. J. Mech. A Solid 25 (6) (2006) 996–1008.
[63] L.Q. Chen, X.D. Yang, Nonlinear free transverse vibration of an axially moving beam: comparison of two models, J. Sound Vib. 299 (1) (2007) 348–354.
[64] J.R. Chang, W.J. Lin, C.J. Huang, S.T. Choi, Vibration and stability of an axially moving Rayleigh beam, Appl. Math. Model. 34 (6) (2010) 1482–1497.
[65] C.W. Lim, C. Li, J.L. Yu, Dynamic behaviour of axially moving nanobeams based on nonlocal elasticity approach, Acta Mech. Sin. 26 (5) (2010) 755–765.

[66] K. Kiani, Longitudinal, transverse, and torsional vibrations and stabilities of axially moving single-walled carbon nanotubes, Curr. Appl. Phys. 13 (8) (2013) 1651–1660.
[67] K. Kiani, Longitudinal and transverse instabilities of moving nanoscale beam-like structures made of functionally graded materials, Compos. Struct. 107 (2014) 610–619.
[68] Y. Fu, J. Zhang, Y. Jiang, Influences of the surface energies on the nonlinear static and dynamic behaviors of nanobeams, Physica E 42 (9) (2010) 2268–2273.
[69] P. Lu, L.H. He, H.P. Lee, C. Lu, Thin plate theory including surface effects, Int. J. Solids Struct. 43 (16) (2006) 4631–4647.
[70] S.P. Timoshenko, On the correction for shear of the differential equation for transverse vibrations of prismatic bars, Philos. Mag. J. Sci. 41 (245) (1921) 744–746.
[71] W.B. Bickford, A consistent higher order beam theory, Dev. Theor. Appl. Mech. 11 (1982) 137–150.
[72] J.N. Reddy, A simple higher-order theory for laminated composite plates, J. Appl. Mech. 51 (1984) 745–752.
[73] J.N. Reddy, Nonlocal theories for bending, buckling and vibration of beams, Internat. J. Engrg. Sci. 45 (2) (2007) 288–307.
[74] J. He, C.M. Lilley, Surface effect on the elastic behavior of static bending nanowires, Nano Lett. 8 (7) (2008) 1798–1802.